The EMBO Journal Vol.16 No.11 pp.3256–3271, 1997

Mex67p, a novel factor for nuclear mRNA export, binds to both poly(A)$^+$ RNA and nuclear pores

Alexandra Segref, Kishore Sharma[1], Valérie Doye[2], Andrea Hellwig, Jochen Huber[3], Reinhard Lührmann[3] and Ed Hurt

University of Heidelberg, BZH, Im Neuenheimer Feld 328, D-69120 Heidelberg, Germany, [1]EMBL, Meyerhofstrasse 1, D-69117 Heidelberg, Germany, [2]Institut Curie, Section de recherche, CNRS UMR144, 2 rue Lhomond, F-75231 Paris Cedex 05, France and [3]Institut für Molekularbiologie und Tumorforschung, Philipps-Universität Marburg, Emil-Mannkopf-Strasse 2, D-35037 Marburg, Germany

An essential cellular factor for nuclear mRNA export called Mex67p which has homologous proteins in human and *Caenorhabditis elegans* was identified through its genetic interaction with nucleoporin Nup85p. In the thermosensitive mex67-5 mutant, poly(A)$^+$ RNA accumulates in intranuclear foci shortly after shift to the restrictive temperature, but NLS-mediated nuclear protein import is not inhibited. *In vivo*, Mex67p tagged with green fluorescent protein (GFP) is found at the nuclear pores, but mutant mex67-5–GFP accumulates in the cytoplasm. Upon purification of poly(A)$^+$ RNA derived from of UV-irradiated yeast cells, Mex67p, but not nucleoporins Nup85p and Nup57p, was crosslinked to mRNA. In a two-hybrid screen, a putative RNA-binding protein with RNP consensus motifs was found to interact with the Mex67p carboxy-terminal domain. Thus, Mex67p is likely to participate directly in the export of mRNA from the nucleus to the cytoplasm.

Keywords: hnRNP/mRNA/nuclear pore complex/ nucleocytoplasmic transport/RNA export

Introduction

The translocation of molecules across the nuclear membrane occurs through the nuclear pore complexes (Fabre and Hurt, 1994; Görlich and Mattaj, 1996). Different transport routes were identified in the past and a picture is emerging that different transport cargoes use different transport vehicles (Gerace, 1995). For nuclear protein import, the nuclear localization sequence (NLS)–receptor complex consisting of importin/karyopherin α and β subunits binds to the NLS of karyophilic proteins in the cytoplasm (Görlich and Mattaj, 1996), followed by a docking step at the nuclear pore complexes, most likely at FXFG or GLFG repeat sequence containing nucleoporins (Rexach and Blobel, 1995). The translocation of the nuclear protein through the nuclear pore channel is then initiated by GTP hydrolysis, mediated by the small GTPase Ran/TC4 (Moore and Blobel, 1993).

RNA export from the nucleus into the cytoplasm is also a signal- and receptor-mediated process (Görlich and Mattaj, 1996). Some of the players participating in the molecular events during RNA export have been recently identified; however, the underlying mechanisms of RNA export remain largely unknown. A cap-binding complex (CBP) which recognizes the monomethylated 5′-end of snRNAs and mRNAs has been shown to mediate U snRNA nuclear export (Izaurralde *et al.*, 1995). Similar to the NLS found in karyophilic proteins, nuclear export sequences (NESs) were recently found in several proteins which shuttle between the nucleus and the cytoplasm (Gerace, 1995). In most cases, these NES-containing proteins are RNA-binding proteins and thus could be involved in the nuclear export of their cognate cargo RNA. This was most convincingly shown for the HIV Rev protein which associates with viral mRNA (Fischer *et al.*, 1994; Bogerd *et al.*, 1995; Stutz *et al.*, 1995) and the hnRNP A1 protein which is bound to mRNA (Michael *et al.*, 1995). HIV Rev transports unspliced and partially spliced viral mRNA from the nucleus into the cytoplasm, and it is the NES of Rev which retargets viral mRNA directly to a cellular export pathway bypassing the splicing machinery (Fischer *et al.*, 1995). Whereas the NES in HIV Rev, PKI (protein kinase inhibitor) and TFIIIA is short (~10 amino acids in length) and leucine-rich with a typical spacing of the hydrophobic residues (Gerace, 1995), the NES of hnRNP A1 (called M9) is significantly longer and does not conform to this consensus (Michael *et al.*, 1995). Interestingly, the M9 sequence also exhibits NLS activity and was recently shown to interact with a novel import receptor called transportin, which is an importin/karyopherin β homologue (Pollard *et al.*, 1996). Since NESs can induce rapid export of attached passenger proteins (Fischer *et al.*, 1995), a search was undertaken for cellular receptors interacting with the nuclear export signal. By using the yeast two-hybrid system, two related proteins from human and yeast (called hRip and Rip1p, respectively), were identified which specifically interact with the HIV Rev NES (Bogerd *et al.*, 1995; Fritz *et al.*, 1995; Stutz *et al.*, 1995). Interestingly, these Rip proteins share similarity to FG repeat-containing nucleoporins which are also candidates for NES receptors that could facilitate transport of Rev-associated RNPs through the NPC (Stutz *et al.*, 1996). Interestingly, yeast Rip1p is not essential for cell growth, suggesting that additional NES receptors must exist in the cell which are essentially involved in RNA export reactions or have overlapping function. Recently, an essential RNA-export mediator called Gle1p which contains a nuclear export signal and interacts with Rip1p and Nup100p has been identified in yeast (Murphy and Wente, 1996). Gle1p is identical to Rss1p (Del Priore *et al.*, 1996) and Brr3p (Noble and Guthrie, 1996) which have been recently found in other genetic screens.

A complementary approach has been undertaken in the yeast *Saccharomyces cerevisiae*, exploiting its powerful genetics, to dissect the nucleocytoplasmic transport

machinery (for review, see Doye and Hurt, 1995). In a genetic screen, a collection of temperature-sensitive mutants was analysed by *in situ* hybridization for nuclear accumulation of poly(A)$^+$ RNA. Many of the obtained mutants, called *rat* (mRNA trafficking) and *mtr* (mRNA transport) mutants (Amberg *et al.*, 1992; Kadowaki *et al.*, 1992), were blocked in nuclear mRNA export. Among the cloned *RAT* and *MTR* genes, some of them encode nuclear pore proteins (Doye *et al.*, 1994; Heath *et al.*, 1995; Li *et al.*, 1995). In particular, *RAT7/NUP159* (Gorsch *et al.*, 1995) and *MTR2* (Kadowaki *et al.*, 1994) are promising candidates for a direct involvement in mRNA export reactions, since thermosensitive mutants show an intranuclear mRNA accumulation shortly after shift to the restrictive temperature. The yeast homologue of RCC1 (the guanine dinucleotide exchanger of Ran) has also been found in such a genetic screen, suggesting that Ran is involved in nuclear RNA export (Kadowaki *et al.*, 1993); similarly, mammalian RCC1 was shown to be required for nuclear RNA export (Cheng *et al.*, 1995). Furthermore, hnRNP proteins in yeast such as Npl3p, which shuttle between the nucleus and the cytoplasm, were also suggested to mediate mRNA export (Lee *et al.*, 1996).

Genetic screens in yeast based on synthetic lethality have proven to be extremely useful in identifying a vast number of nuclear pore complex proteins with roles in nuclear pore biogenesis, nuclear pore structure and/or nucleocytoplasmic transport (Doye and Hurt, 1995). Among the many nucleoporins identified so far, some appear to have distinct roles in nuclear protein import, mRNA export and tRNA export, respectively (Simos *et al.*, 1996). Other nucleoporin mutants not only have defects in nucleocytoplasmic transport reactions, but possess exhibit structural abnormalities of the nuclear envelope and NPCs (Doye and Hurt, 1995), making it difficult to assign the primary defect. Furthermore, in many of these nucleoporin mutants the manifestation of transport defects was not immediate after shifting cells to the restrictive condition, making it likely that observed transport defects could be pleiotropic.

Recently, a novel nucleoporin complex consisting of Nup120p, Nup85p, Nup84p, band IV, Sec13p and a Sec13 homologue (Seh1p) was identified in yeast and plays roles in coordinated nuclear membrane/NPC biogenesis and in nuclear export of mRNA and tRNA (Siniossoglou *et al.*, 1996). We used a mutant of one member of this complex, Nup85p, which exhibits a poly(A)$^+$ RNA export defect, to search for novel factors involved in nuclear mRNA export. Here, we report the identification of such a component, called Mex67p, which is essential for mRNA transport out of the nucleus. Our studies indicate that Mex67p is likely to be involved in nuclear mRNA export mechanisms.

Results

A synthetic lethal screen with a mutant allele of NUP85 identifies the essential mRNA export factor Mex67p

A nucleoporin complex of six proteins which includes Nup85p is required for nuclear pore biogenesis and RNA export (Siniossoglou *et al.*, 1996). Interestingly, a nup85 null mutant is impaired in both NPC organization and RNA export, whereas cells which express an amino-terminally truncated Nup85p (nup85Δ) and are thermosensitive for growth at 37°C are mainly defective in poly(A)$^+$ RNA export (Siniossoglou *et al.*, 1996). This observation prompted us to perform a synthetic lethal (sl) screen with the *nup85*Δ allele to identify novel components of the mRNA export machinery (see Materials and methods). In total, 13 sl mutants were isolated which are synthetically lethal with *nup85*Δ, but not with *NUP85*. The wild-type gene of a *NUP85* interacting component was cloned by complementation of one of these sl mutants (sl102) with a yeast genomic library. The complementing activity was restricted to an uncharacterized yeast gene on chromosome XVI, which encodes a putative protein of 599 amino acids (Figure 1A). The deduced molecular weight of this novel protein is 67.351 kDa. Since this protein plays an essential role in mRNA export (see also later), it was named Mex67p and its gene *MEX67* (for Messenger RNA EXport factor of 67 kDa molecular weight). A search in protein sequence data libraries for putative higher eukaryotic homologues of yeast Mex67p (accession No. Z73525) revealed three sequences with significant homology and a similar domain organization (Figure 1A and B); one is a human protein called TAP (accession No. D42085) and the other two are uncharacterized ORFs from *C.elegans* (accession Nos: C15H11.e/e275614; C15H11.d/e275615).

Disruption of the *MEX67* gene showed that it is essential for cell growth (data not shown). In order to study the *in vivo* role of Mex67p, thermosensitive mutants were generated by random mutagenesis of the isolated *MEX67* gene. Among the three thermosensitive mutants obtained, ts mex67-5 was chosen for further analysis, because it showed no apparent growth defect at 30°C, but completely stopped cell growth shortly after shifting the cells to 37°C (Figure 2A and B). This suggests that an essential cellular process is tightly controlled by Mex67p. Interestingly, ts mex67-5 cells only arrest, but do not die at 37°C, which can be observed by the reversibility of the ts phenotype. Even after prolonged incubation of ts mex67-5 cells at 37°C (e.g. 12 h), >50% of the cells are viable and can regrow if brought back to 30°C (Figure 2C). Thus, *mex67-5* is a thermoreversible ts allele. The mutation causing the ts phenotype in mex67-5 is due to a single amino acid exchange, His400 to Tyr400 (Figure 1A).

MEX67 was isolated on the basis of synthetic lethality with the mutated *nup85*Δ gene. When strain sl102 was transformed with plasmid-borne *MEX67* alleles, synthetic lethality was only complemented at 30°C by intact *MEX67*, but not *mex67-5* (data not shown). Furthermore, a haploid yeast strain was constructed in which the *nup85*Δ and the ts *mex67-5* allele were combined, but this strain was not viable when the pURA3–MEX67 plasmid was shuffled out on 5-fluoro-orotic acid (FOA) plates (data not shown). This demonstrates synthetic lethality between the two mutant alleles. When we analysed whether *MEX67* is also linked to other members of the Nup85p complex or to other nucleoporins, no synthetic lethality was seen below 30°C between *mex67-5* and mutant alleles of *nup84*, *seh1* and *pom152* (see Materials and methods). However, the combination of *mex67-5* and *nup84::HIS* caused synthetic lethality at 33°C, a temperature at which the single mutants are still able to grow (data not shown). This genetic analysis thus revealed a strong genetic overlap between *MEX67* and *NUP85*, and a weaker or no genetic interaction

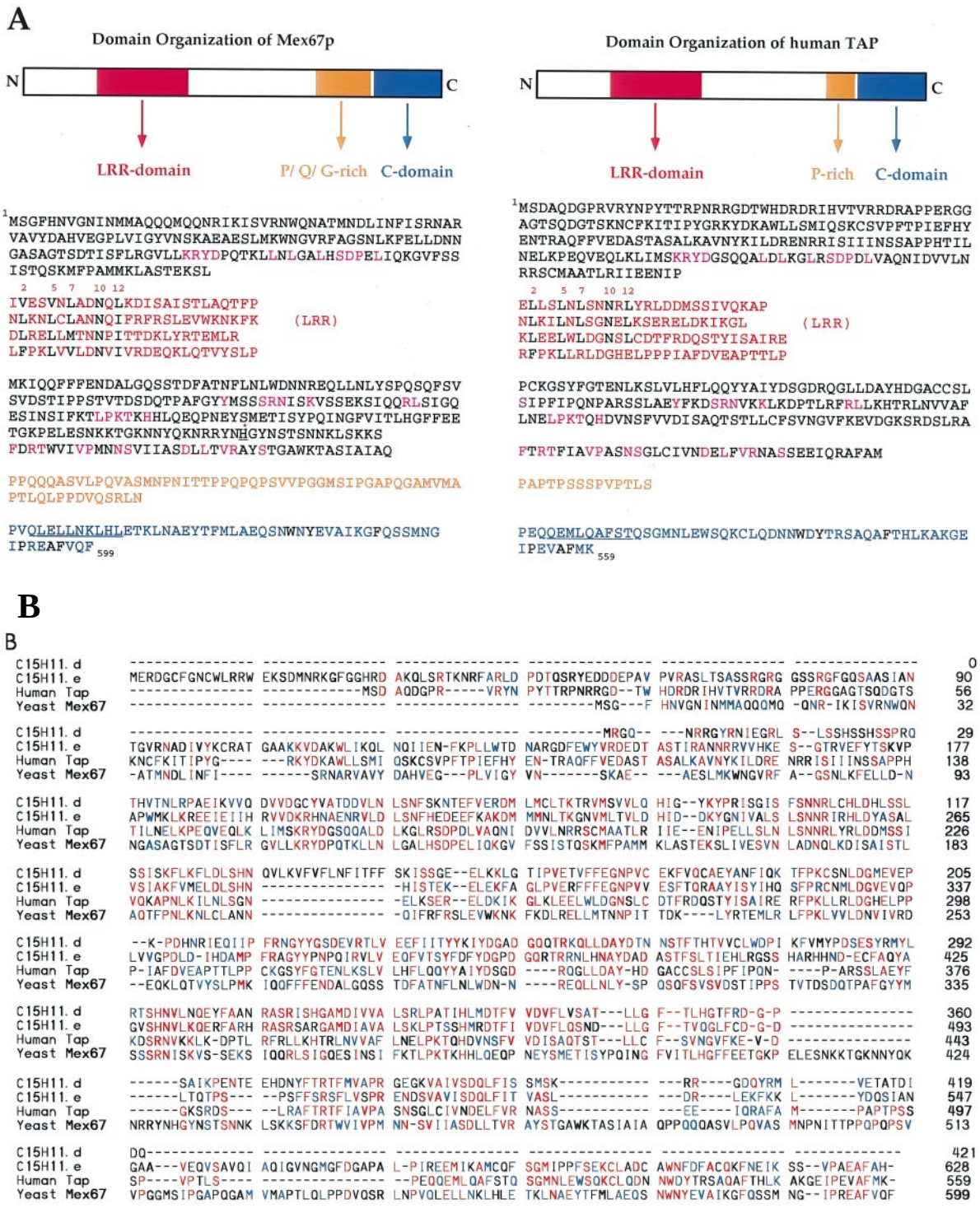

Fig. 1. Structural organization and homology of Mex67p. (**A**) Domain organization and primary amino acid sequence of Mex67p and a homologous human protein called TAP (accession No. U80073). The various domains are highlighted with different colours including a Leucine-Rich Repeat (LRR)-domain (red), an uncharged proline/glutamine/glycine-rich sequence (orange) and the carboxy-terminal domain (blue). The LRR domain was aligned in a way that the four LRRs become evident. Conserved residues in the LRRs are at position 2, 5, 7, 10 and 12 and shown in black. LRRs occur in several other proteins including the ribonuclease inhibitor whose crystal structure has been recently solved. It was speculated that the LRR is involved in protein–protein interactions (Kobe and Deisenhofer, 1994). Within the Mex67p carboxy-terminal domain, a short sequence is underlined, which resembles the HIV Rev NES. The point mutation H(400) to Y in ts *mex67-5* is indicated by a star. (**B**) Multiple sequence alignment of Mex67p with human TAP (accession No. U80073), and two *C.elegans* ORFs (C15H11.e/e275614; C15H11.d/e275615) using ClustalW1.6 (BCM Search Launcher).

with mutant alleles of *NUP84*, *SEH1* and *POM152*, respectively.

Since *MEX67* was found in conjunction with the *nup85*Δ mutant allele which causes poly(A)$^+$ RNA to accumulate inside the nucleus, we tested whether Mex67p on its own participates in mRNA export. By *in situ* hybridization using a FITC-labelled oligonucleotide poly(dT)$_{50}$ probe, poly(A)$^+$ RNA was localized in the cytoplasm of mex67-5

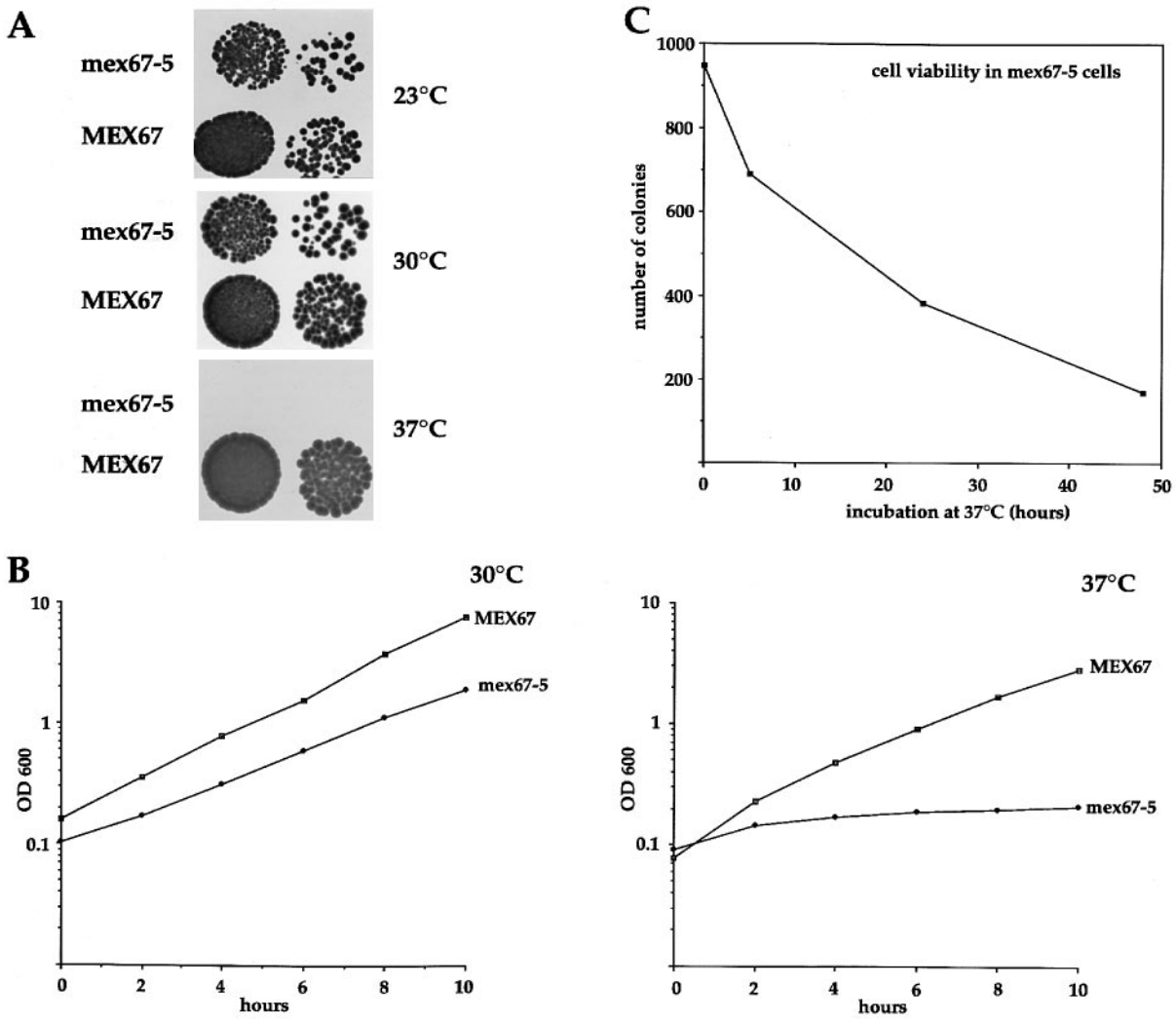

Fig. 2. A reversible temperature-sensitive mutant of Mex67p. (**A**) Growth of mutant mex67-5 and wild-type MEX67 cells at different temperatures. Precultures were diluted in liquid YPD medium and equivalent amounts of cells (undiluted or 1/10 diluted) were spotted onto YPD plates. Plates were incubated for 3 days at 23°C and 30°C, and for 3 days at 37°C. (**B**) Growth curves of wild-type MEX67 and temperature-sensitive mex67-5 strains in YPD liquid medium at 30°C or 37°C. Cell growth was followed by measuring the optical density at 600 nm (OD_{600}). (**C**) Cell viability of mex67-5 cells incubated at the restrictive condition. For each time point, the same number of mex67-5 cells (~1000 per plate) were plated on a YPD-plate. Plates were incubated at 37°C for the indicated time points, before being brought back to 30°C. The number of colonies which formed after 3 days at 30°C were determined.

cells if grown at the permissive temperature (Figure 3A). After shifting the cells for 15–30 min to 37°C, however, poly(A)$^+$ RNA strongly accumulated inside the nucleus in almost all of the mex67-5 cells (Figure 3A). Strikingly, this intranuclear RNA was concentrated in several discrete spots which varied in number (Figure 3A and B). Concomitantly, the nucleolar marker Nop1p was also changed in its distribution in the ts mex67-5 mutant, becoming clustered in several intranuclear spots (Figure 3B). Disintegration of the nucleolus was frequently observed in nucleoporin mutants including nup85 (Goldstein *et al.*, 1996) and nup120 mutants (Aitchison *et al.*, 1995b; Heath *et al.*, 1995). However, the spots containing Nop1p did not co-localize with the accumulated poly(A)$^+$ RNA (Figure 3B), as opposed to two other mRNA export mutants, in which nucleolar antigens and mRNA co-localize inside the nucleus (Kadowaki *et al.*, 1994). In contrast, the distribution of nuclear pore antigens was normal in mex67-5 cells with no tendency of NPC clustering (see also later). It thus appears that, in ts mex67-5 cells, polyadenylated RNA accumulates in discrete intranuclear foci which are not in close contact with the nuclear pore complexes. To determine whether the mex67-5 mutant exhibits morphological abnormalities of the nuclear envelope at the ultrastructural level, thin-section electron microscopy was performed. In ts mex67-5 cells shifted to 37°C, nuclear envelope and NPC morphology, as well as NPC number appeared normal, as judged from the inspection of electron micrographs (Figure 4); however, numerous electron-dense aggregates were seen in the ts mex67-5 mutant incubated at the restrictive temperature (Figure 4, arrows; see also Discussion). In addition, fragmentation of the nucleolus, which can be easily identified because of its typical fibrillar-like appearance, was also visible by electron microscopy (Figure 4, arrowheads).

It was further tested whether the biogenesis of other RNA species is altered in ts mex67-5 cells. When rRNA

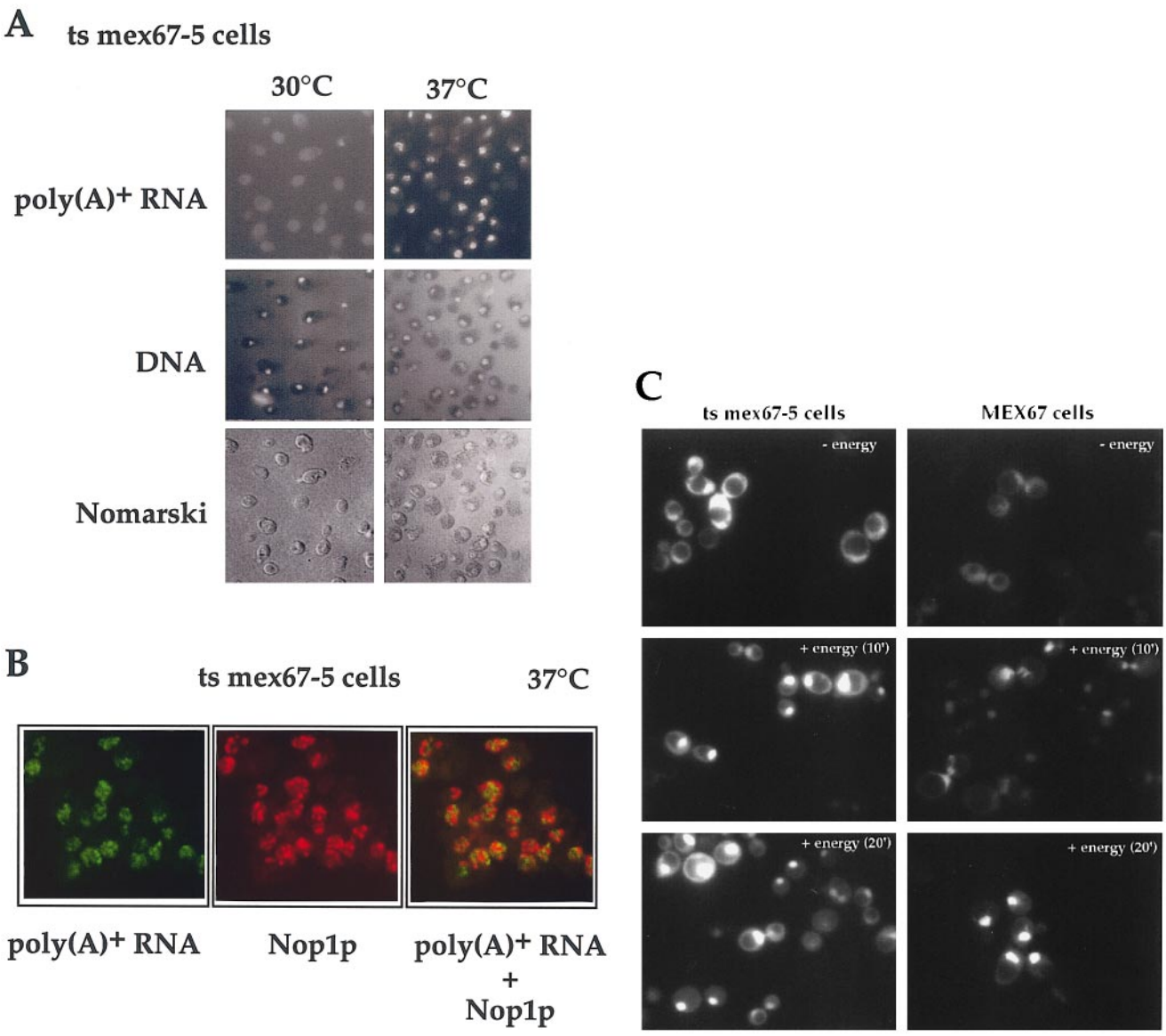

Fig. 3. Analysis of nuclear RNA export of nuclear protein import in mex67-5 cells. (**A**) Accumulation of polyadenylated RNA in the nucleus of ts mex67 cells. Subcellular localization of poly(A)$^+$ RNA was analysed by *in situ* hybridization with a FITC-labelled oligonucleotide poly(dT) probe. Ts mex67-5 cells were either grown at 30°C or shifted for 30 min to 37°C in YPD-medium. Nuclear DNA was stained by Hoechst 33258 and cells were viewed by Nomarski optics. (**B**) The fragmented nucleolus does not co-localize with accumulated polyadenylated RNA in ts mex67-5 cells. Thermosensitive mex67 cells were shifted for 30 min to 37°C before cells were fixed and processed for both, *in situ* hybridization with oligo(dT)-FITC [poly(A)$^+$ RNA] and indirect immunofluorescence using anti-Nop1p antibodies (Nop1p). Both pictures which were obtained from the confocal microscope were merged [poly(A)$^+$ RNA + Nop1p], indicating that poly(A)$^+$ and Nop1p-clusters generally do not co-localize. (**C**) Analysis of nuclear protein import in ts mex67-5 cells. Intracellular location of the NLS–GFP reporter protein in ts mex67 and MEX67 cells as revealed by fluorescence microscopy. Cells were preincubated for 1 h at 37°C before the *in vivo* nuclear import analysis was performed essentially after Shulga *et al.* (1996). – energy: indicates that cells were treated with azide and deoxyglucose. + energy (10′) and + energy (20′), cells after recovery from the drug treatment in glucose-containing medium for 10 and 20 min, respectively. Note that nuclear re-import of GFP–NLS which leaked out into the cytoplasm in energy-depleted cells, is almost complete after 10 min of re-energization, both in mex67-5 and MEX67$^+$ cells.

processing was analysed by Northern analysis (Tollervey *et al.*, 1993), no significant impairment of pre-rRNA processing was seen in ts mex67-5 cells after a 30 min shift to 37°C; however after prolonged incubation (e.g. 1 h) at 37°C, a decrease of the 32S and 27SA2 pre-rRNA species, and the simultaneous appearance of the 23S precursor, was noticed. Processing of 20S to mature 18S rRNA, however, was not affected (data not shown). Accordingly, pre-rRNA processing occurs at 37°C in the mex67-5 mutant, but a delay in the cleavage at site A0, A1 and A2 can be measured at later time points of restrictive incubation. Processing and transport of tRNA was normal, since no defect in tRNA splicing and no loss of suppressor tRNA activity was observed in the mex67-5 mutant (data not shown). Finally, mRNA splicing was also not inhibited in the mex67-5 mutant when shifted to 37°C, as seen by the fact that no intron-containing actin mRNA was found (data not shown).

To determine whether nuclear protein import is inhibited in ts mex67-5 cells, we tested the nuclear import of the karyophilic reporter protein Matα2–lacZ (Nehrbass *et al.*, 1993); however, no cytoplasmic accumulation was found at the restrictive temperature (data not shown). Since poly(A)$^+$ RNA export is efficiently inhibited in ts mex67-5

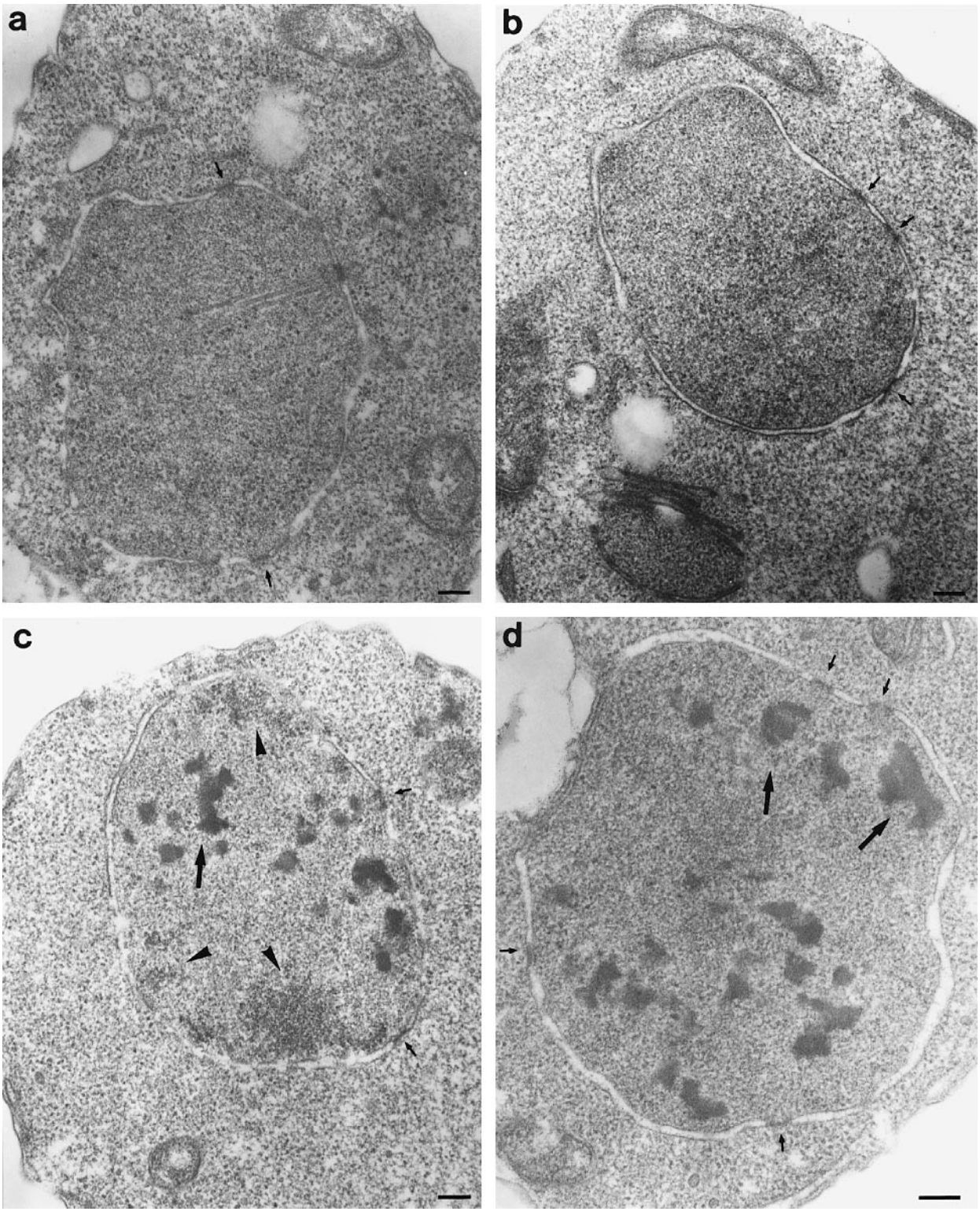

Fig. 4. Electron microscopic analysis of ts mex67-5 cells. Wild-type MEX67 and ts mex67-5 cells were grown to the early logarithmic phase at 30°C or 37°C before processing them for thin-section electron microscopic analysis as described under Materials and methods. (**a**) Wild-type MEX67 cells grown for 2 h at 37°C; (**b**) ts mex67-5 cells, grown at 30°C; (**c** and **d**) ts mex67-5 cells grown for 2 h at 37°C. Small arrows point to nuclear pores, large arrows to electron-dense intranuclear aggregates, which most likely are hRNP clusters, and arrowheads to the fragmented nucleolus. Bar, 0.2 μm.

cells, one can not exclude that the nuclear reporter protein is no longer synthesized at the restrictive temperature due to the cytoplasmic depletion of reporter mRNA. Therefore, we used a recently developed assay for *in vivo* nuclear protein import which does not depend on ongoing mRNA synthesis and export (Shulga *et al.*, 1996). In this assay, cells which express and accumulate a NLS–GFP reporter protein inside the nucleus are first poisoned with inhibitors of energy metabolism. This causes leakage of NLS–GFP into the cytoplasm. After washing and resuspending the

cells in glucose-containing medium, normal ATP levels are restored, allowing rapid nuclear re-import of NLS–GFP. When the ts mex67-5 mutant expressing NLS–GFP was shifted for 1 h to 37°C and then analysed according to this assay, no defect in nuclear re-import of the NLS–GFP reporter protein was seen as compared with wild-type cells (Figure 3C). In summary, the early onset of an mRNA export defect in ts mex67-5 mutant cells with no apparent impairment in NLS-mediated nuclear protein import suggests that Mex67p is directly involved in nuclear mRNA export reactions.

Mex67p is a nuclear pore-associated protein which accumulates in the cytoplasm in ts mex67 cells

The functional interaction of Mex67p with nucleoporins and its essential role in nuclear mRNA export suggests that the protein might be localized at the nuclear pores. Therefore, Mex67p was tagged at its carboxy-terminal end with different epitopes derived from Protein A or the Green Fluorescent Protein (see Materials and methods). These fusion proteins were functional since they could complement the lethal phenotype of the mex67 null mutant if expressed from yeast single-copy plasmids (data not shown). Mex67p–ProtA showed a punctuate nuclear envelope staining in wild-type cells and co-clustering with nuclear pore antigens in nup133^{-} cells (data not shown). Also, the *in vivo* location of GFP-tagged Mex67p was predominantly at the nuclear pores, as seen by the ring-like and punctuate staining of the nuclear envelope (Figure 5A). This staining closely resembles the *in vivo* labelling seen with a bona fide nucleoporin, NUP49–GFP (Belgareh and Doye, 1997). Finally, the fluorescence signals from Mex67–GFP and Nsp1p largely overlapped, as revealed by double immunofluorescence microscopy (data not shown). Thus, under steady-state conditions, Mex67p shows a preferential location at the nuclear pores.

A different intracellular location was seen when the mutant protein mex67-5p tagged with GFP was analysed by fluorescence microscopy; mex67-5–GFP complemented the lethal phenotype of the mex67 null disruption mutant at permissive temperatures, but cells were thermosensitive for growth at 37°C (data not shown). When cells were grown at 23°C, mex67-5–GFP was found predominantly at the nuclear envelope; however, this location changed when cells were shifted for as little as 5–10 min to 37°C (Figure 5B). The mex67-5–GFP fusion protein was no longer associated with the nuclear envelope, but detached from the nuclear pores and appeared in many dot-like structures scattered throughout the cytoplasm. When the mutant was reshifted to 23°C, the cytoplasmic clusters disappeared and the nuclear envelope staining often resumed. Wild-type Mex67–GFP did not show this behaviour and was always found at the NPCs, even at 37°C (Figure 5B). To determine whether the cytoplasmic localization of ts mex67-5–GFP seen at 37°C is due to a general dissociation of nucleoporins from the nuclear pores, double indirect immunofluorescence of fixed and spheroplasted ts mex67-5–GFP cells was performed using anti-nucleoporin antibodies. Thermosensitive mex67-5–GFP accumulated in dot-like cytoplasmic structures, whereas nucleoporins recognized by the monoclonal antibody Mab414 remained associated with the NPCs (data not shown). We next tested whether ProtA–Nup85p becomes mislocalized in ts mex67-5 cells shifted for 1 h to 37°C, but again this nucleoporin remained exclusively bound at the NPCs. Finally, Mex67p–GFP was strictly found at the nuclear pores in nup85Δ mutant cells, shifted for 2 h to the restrictive temperature (data not shown). Taken together, these data show that mutated mex67-5–GFP, but not other nucleoporins, dissociates from the nuclear pores into the cytoplasm under restrictive conditions and is retargeted to the nuclear envelope when shifted to permissive temperature.

A short sequence in the carboxy-terminal domain is essential for in vivo function of Mex67p

The sequence ^{549}LELLNKLHL^{557} in the carboxy-terminal domain of Mex67p resembles the NES of HIV Rev (Figure 6A; see also Figure 1A). We therefore coupled this NES-resembling peptide (CLEL**L**NKLHL) and a mutant form (CLEL**P**NKLHL; see also later) to ^{125}I-labelled bovine serum albumin (BSA) and microinjected the conjugates into *Xenopus* oocyte nuclei. The NES-mediated export was then followed by: (i) determining the amount of Mex67p NES–BSA in the nucleus and cytoplasm; and (ii) measuring competition of Rev-mediated RNA export in the presence of Mex67p NES–peptides coupled to BSA. The NES-like sequence of Mex67p, but not its mutant form, exhibits a nuclear export activity in the *Xenopus* oocyte system which is comparable in its efficiency to the activity of the Rev NES (Figure 7A). Furthermore, the Rev-mediated export of pAd46 RNA, harbouring the Rev-responsive element (RRE), and export of U1ΔSm RNA were also competitively inhibited by intact, but not mutated Mex67p NES–BSA (Figure 7B). This showed that the NES-like sequence of Mex67p exhibits a nuclear export activity in the *Xenopus* oocyte system, but it is uncertain whether this sequence also has NES-activity in the context of the native Mex67p protein (see also Discussion).

To find out about the *in vivo* role of this short sequence, it was deleted from Mex67p; however, yeast cells were not viable (Figure 6B, left panel). Therefore, more subtle mutations were made (Figure 6A). Whereas the L(552)→E mutation only partially impairs the *in vivo* function of Mex67p (i.e. yeast cells grow more slowly, particularly at 37°C as compared with wild-type cells; see also Figure 6B, right panel), the L(552)→P mutation no longer allows cell growth at any temperature (Figure 6B, left panel). Thus, single amino acid exchanges in this short sequence can impair the *in vivo* function of Mex67p. Furthermore, RNA export was inhibited in these mutant cells (data not shown).

To test whether the mutations in the NES-like sequence affect the intracellular location, the Mex67p [L→E] construct and another mutant, Mex67p [LL→EE] (see also Figure 6A) were GFP-tagged and expressed in the mex67 null mutant. Also the Mex67p [LL→EE]–GFP construct is functional at permissive temperatures (e.g. at 30°C), but cells grow more slowly as compared with Mex67p [L→E]–GFP cells (data not shown). In the fluorescence microscope, these two GFP-tagged mutant proteins no longer revealed a distinct nuclear envelope staining but, instead, an increased cytoplasmic labelling. Moreover, an intranuclear accumulation of Mex67p could also be seen in a few cells (Figure 6C). In contrast, wild-type Mex67–GFP and ts mex67-5–GFP were seen predominantly at

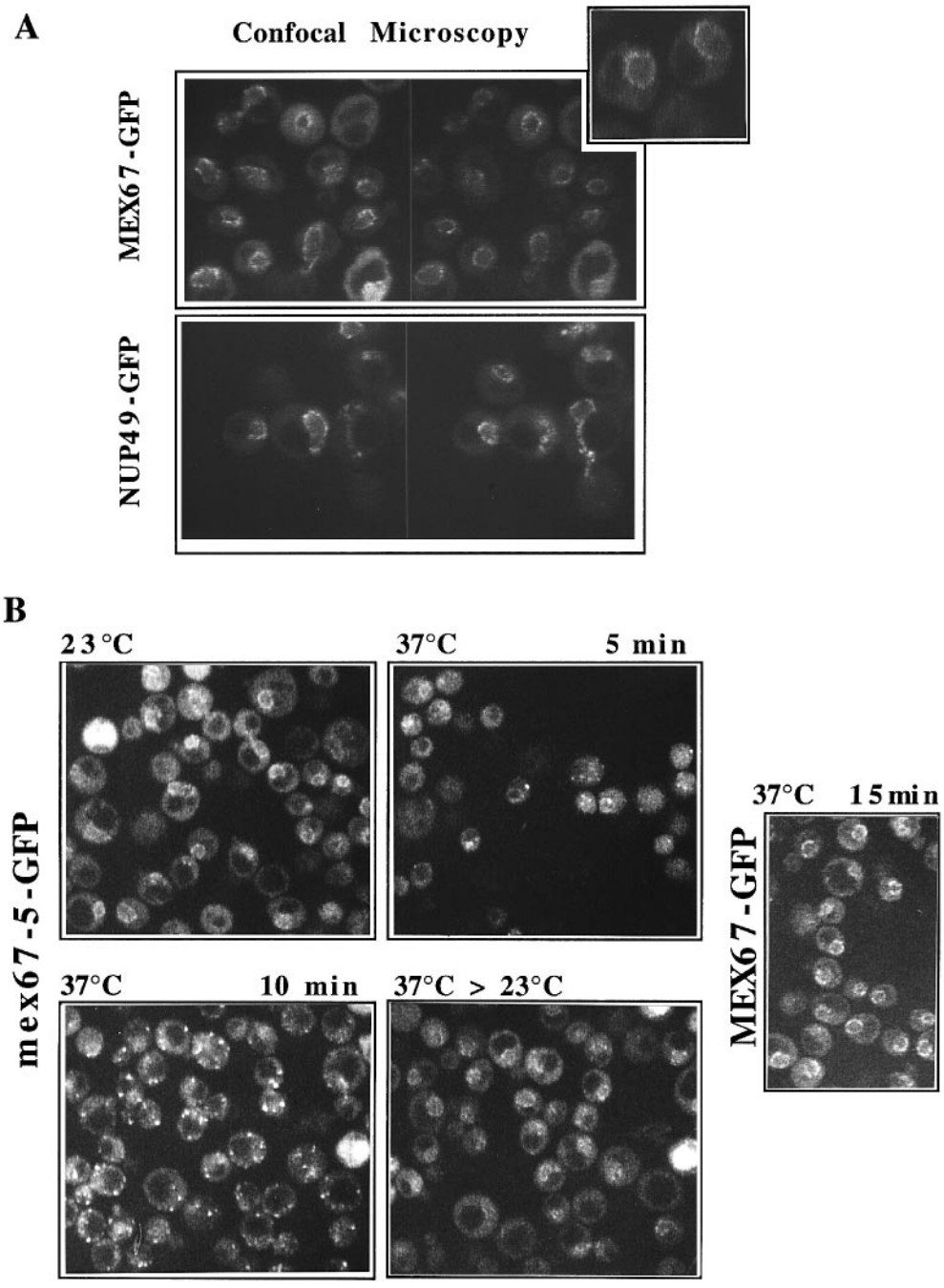

Fig. 5. Localization of GFP-tagged Mex67p in living cells. (**A**) Confocal fluorescence microscopy of living MEX67–GFP cells. Two successive sections, each 0.5 μm thick, are shown for MEX67–GFP, and for comparison, NUP49–GFP cells. The insert shows a higher magnification of MEX67–GFP cells which reveals a typical nuclear pore labelling, with little staining in the nucleoplasm and cytoplasm, and no staining inside the vacuole. (**B**) Confocal fluorescence microscopy of thermosensitive mex67-5–GFP cells. Living cells growing for the indicated time periods and temperatures in liquid medium were inspected in the confocal fluorescence microscope. The same mex67-5–GFP cells which were immobilized on the microscopic slide, were viewed and photographed twice, once after 10 min shift to 37°C and a second time after a 20 min reshift to 23°C. For control reasons, also MEX67–GFP cells were grown for 15 min at 37°C.

the nuclear envelope under these conditions (Figure 6C). Strikingly, Mex67p [L→E]–GFP and Mex67p [LL→EE]–GFP cells exhibit a significantly increased cell size (Figure 6C).

Mex67p binds to poly(A)$^+$ RNA

Since Mex67p participates in RNA export, we tested whether Mex67p is physically associated with poly(A)$^+$ RNA. Since this interaction could be transient and only a minor pool of mRNA may be associated with Mex67p under steady-state conditions (>90% of polyadenylated RNA is found in the cytoplasm; Anderson *et al.*, 1993), yeast cells were UV-irradiated before cell lysis to crosslink bound proteins to RNA prior to purification of polyadenylated RNA. Using this method it has been previously shown that several hnRNP proteins, including Nab1/Npl3/Nop3p, can be photo-crosslinked to poly(A)$^+$ RNA (Anderson *et al.*, 1993; Russell and Tollervey, 1995). When

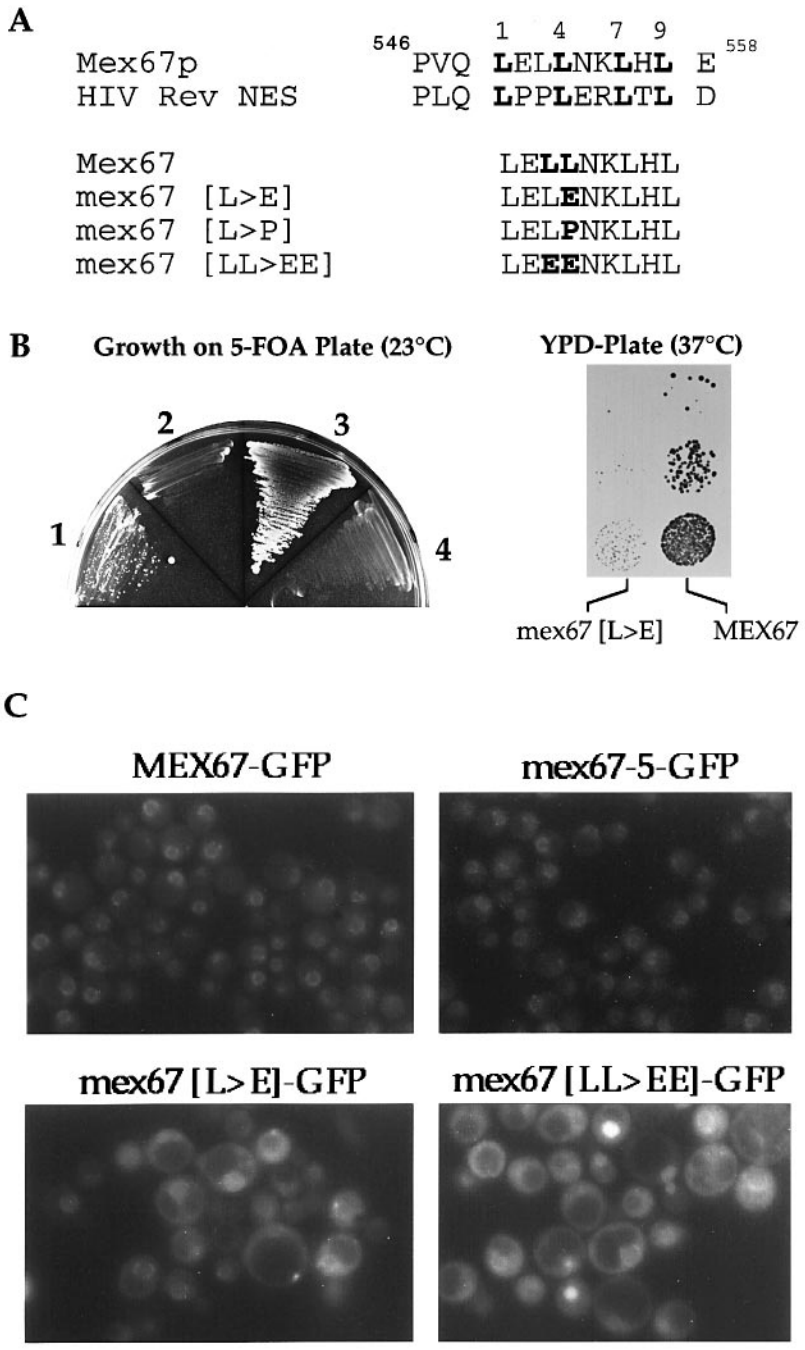

Fig. 6. Mutational analysis of a short essential sequence in the Mex67p carboxy-terminal domain. (**A**) Comparison of HIV Rev NES with a short sequence in the Mex67p carboxy-terminal domain. The conserved leucine residues at position 1, 4, 7 and 9 within the nine amino acid-long NES and flanking residues are shown. Three mutations in the corresponding Mex67p sequence are shown in bold. (**B**) Left panel: strain MEX67 shuffle (mex67::HIS3/pURA3–MEX67) was transformed with pTRP1–mex67 [L→E] (1), pTRP1–mex67–D544-559 (2), pLEU2–MEX67 (3) and pTRP1–mex67 [L→P] (4). Transformants were streaked on a 5-FOA plate and further incubated at 23°C. The plate was grown for 5 days before the picture was taken. Right panel: growth of mex67 [L→E] and MEX67 cells at 37°C was analysed on YPD-plates. (**C**) *In vivo* location of mex67–GFP proteins with mutations in the NES-like motif. Fluorescence microscopy was performed with strains MEX67–GFP, mex67-5–GFP, mex67 [L→E]–GFP and mex67 [LL→EE]–GFP, incubated for 1 h at 30°C. Pictures were taken with a Xillix Microimager CCD camera and exposure times and recording parameters were identical in all cases.

polyadenylated RNA was isolated by oligo(dT)-cellulose chromatography and tested for the presence of Mex67p by Western analysis, Mex67p was clearly UV-crosslinked to poly(A)$^+$ RNA (Figure 8, +UV light). However, the Mex67p band was completely absent from purified poly(A)$^+$ RNA when isolated under the identical conditions from cells which have not been subjected to UV irradiation (Figure 8, –UV light). Similar results were also obtained with the hnRNP protein Nab1p/Npl3p (Figure 8; see also Anderson *et al.*, 1993). On the contrary, the Nop1p band, which served as a well-known negative control (Russell and Tollervey, 1995), was entirely absent from polyadenylated RNA (Figure 8). Finally, when probed for other nucleoporins such as Nup85p and Nup57p, no UV-induced cross-

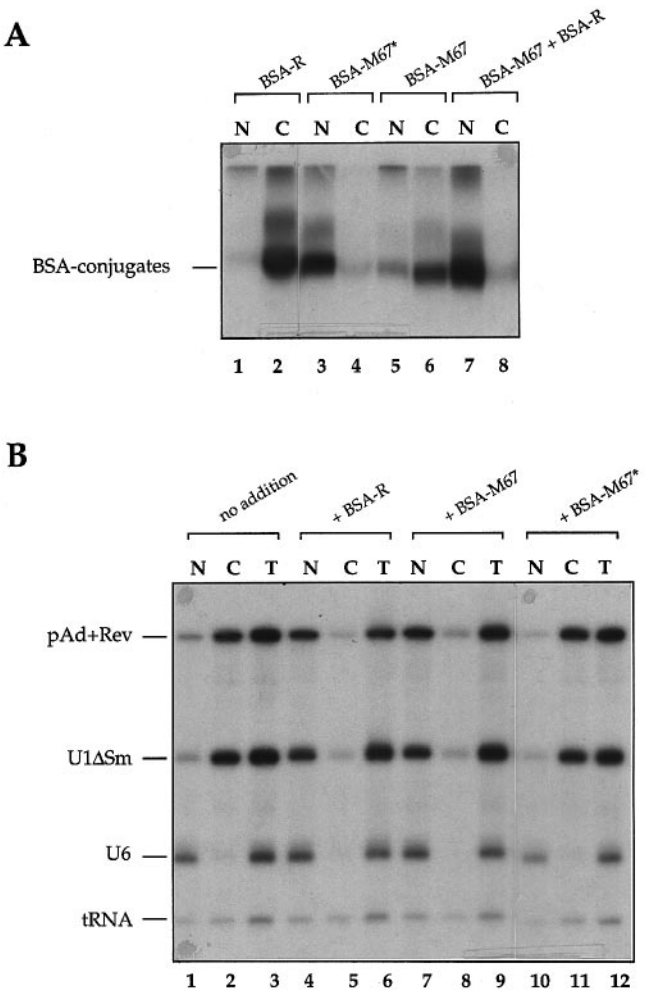

Fig. 7. Mex67p contains a short sequence which exhibits NES-activity in the *Xenopus* oocyte system. (**A**) The NES motif of Mex67p targets BSA to the cytoplasm in *Xenopus laevis* oocytes. ^{125}I-labelled BSA-R (lanes 1 and 2; R is the Rev NES coupled to BSA), BSA-M67* (lanes 3 and 4; M67* is the Mex67p mutant NES peptide coupled to BSA: BSA-CLELPNKLHL), or BSA-M67 (lanes 5 and 6; M67 is the wild-type Mex67p NES peptide coupled to BSA: BSA-CLELLNKLHL) (0.25 mg/ml each) were injected into the nucleus of oocytes alone, or BSA-M67 was injected with a 40-fold molar excess of unlabelled BSA-R (lanes 7 and 8). The nuclear export was analysed 60 min later by protein extraction from nuclear (N) and cytoplasmic (C) fractions and analysis on SDS–polyacrylamide gels. (**B**) Saturation of the Rev-mediated RNA export by BSA-M67. A mixture of ^{32}P-labelled *in vitro* transcribed pAd46 RNA, U1ΔSm RNA (both m^{7}G-capped), U6 snRNA (to monitor nuclear injection) and tRNA was injected into the nucleus of *Xenopus laevis* oocytes along with a 20-fold molar excess of Rev protein either with water (lanes 1–3), BSA-R (lanes 4–6), BSA-M67 (lanes 7–9), or BSA-M67* (lanes 10–12) at concentrations of 10 mg/ml. After the oocytes have been incubated for 90 min at 20°C, the nuclear export was analysed by extracting the RNAs from the nuclear (N), cytoplasmic (C) or both compartments (T) and separation on a denaturing polyacrylamide gel. The injected RNA was detected by autoradiography.

link to poly(A)$^+$ RNA was observed (Figure 8). This shows that Mex67p, in contrast to other tested nucleoporins, is associated with polyadenylated RNA.

Two-hybrid interaction between Mex67p and a putative RNA-binding protein

In an attempt to identify proteins which interact with Mex67p, a two-hybrid screen was performed. Different

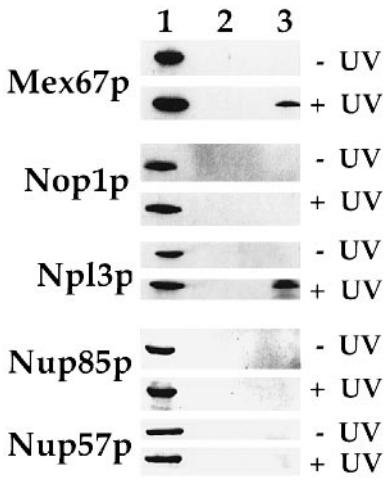

Fig. 8. Mex67p is crosslinked to polyadenylated RNA by UV light. Immunoblot analysis of proteins, which were UV-crosslinked to polyadenylated RNA. Affinity-purified antibodies against Mex67p and Nup85p, and immune sera against Nop1p, Npl3p (Nab1p) and the carboxy-terminal domain of Nup57p were used for the Western blot. 1, Flow-through of a whole cell extract from strain BJ926 which passed over an oligo(dT)-cellulose column; 2, second flow through derived from the prebound first oligo(dT)-cellulose eluate (see Materials and methods); 3, purified poly(A)$^+$ RNA-associated proteins derived from UV-irradiated and not UV-irradiated BJ926 cells, respectively. Only the relevant area of the immunoblot is shown.

Mex67p baits were constructed. Whereas the full-length Mex67p fused to the Gal4p binding domain was expressed at very low levels in the screening strain (data not shown), a construct called pAS2–MEX67 (II) which contained part of the P/Q/G domain plus the entire carboxy-terminal domain (from residue 528–599; see also Figures 1A and 9A) yielded good bait expression and therefore was used in a two-hybrid screen with a yeast genomic library. Among the 1.5×10^6 screened colonies, two Mips (Mex67-interacting protein) were obtained. One clone, *MIP6*, which encodes a putative RNA-binding protein, showed a strong two-hybrid interaction with Mex67p as seen by the formation of blue lacZ$^+$ colonies (Figure 9A, left panel); however, when Los1p (Simos *et al.*, 1996) fused to the Gal4p DNA-binding domain used as a bait, no two-hybrid interaction with Mip6p was seen. Conversely, when pAS2–MEX67 (II) was tested as a bait and pACTII–NUP2 as a prey, no blue colonies formed (Figure 9A, left panel). Mip6p is an uncharacterized ORF in yeast which belongs to the superfamily of RNA-binding proteins (Figure 9B; see also Discussion). The *MIP6* two-hybrid clone is fused to the *GAL4* activating domain at amino acid F(273) which is between the second and third RNP domain (Figure 9B). However, the Mip6p carboxy-terminal domain alone, lacking all RNP domains, can still interact with Mex67p, as seen by the strong two-hybrid interaction between pACTII–Mip6p (385) and pAS2–MEX67 (II) (Figure 9A, right panel). To rule out that an artificial peptide sequence generated at the junction site between the Gal4p DNA-binding domain and Mex67p was the cause for the two-hybrid interaction with Mip6p, two other Mex67p bait constructs were tested: whereas a bait construct containing the entire P/Q/G region plus the carboxy-terminal domain fused to the Gal4p DNA-binding domain [called pAS2–MEX67 (I)] was positive in the two-hybrid assay, another bait construct [pAS2–MEX67

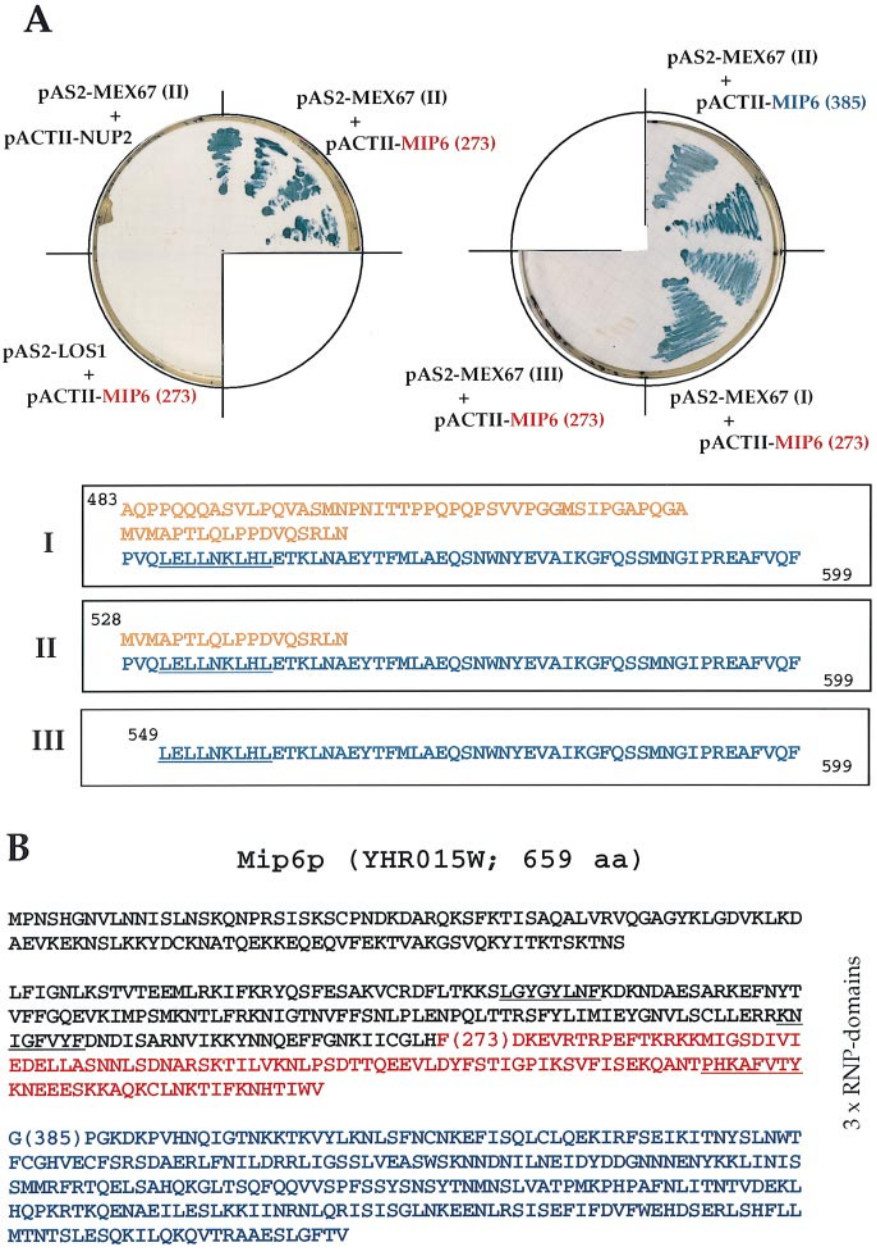

Fig. 9. Two-hybrid interaction between Mex67p and a putative RNA-binding protein. (**A**) Growth and blue colour development on X-Gal plates. Left panel: Re-isolated pACTII–MIP6 (273) plasmid (prey; derived from the two-hybrid screen) was co-transformed with pAS2–MEX67 (II) construct (bait; corresponding to residues 528–599 of Mex67p) into strain Y190 (*gal4*, *gal80*, *trp1*, *leu2*, *his3*, UAS_{GAL}–*LacZ*). For control reasons, other bait/prey combinations were also tested, including pAS2–MEX67 (II)/pACTII–NUP2 and pAS2–LOS1/pACTII–MIP6 (273). In each case, four transformants growing on SDC (–leu –trp) were streaked on SDC (–leu –trp –his; + 15 mM 3-AT; + X-Gal) plates. Right panel: combination of different Mex67p bait and Mip6p prey constructs. (**B**) *MIP6* encodes a putative RNA-binding protein in yeast (accession No. YHR015W, 659 amino acids). The three RNP motifs are underlined. The *MIP6* two-hybrid clone initially isolated from the screen was fused to the *GAL4* activating domain at position F (273). A second construct was made and tested in the two-hybrid assay in which only the C-domain of Mip6p starting at G (385) and lacking the RNP domains was fused to the Gal4p activating domain.

(III)] starting exactly at the NES-like sequence of Mex67p (Figure 9A, right panel) or the P/Q/G domain alone (data not shown) did not exhibit a two-hybrid interaction with Mip6p. Thus, an intact Mex67p carboxy-terminal domain which includes part of the P/Q/G domain is required for the two-hybrid interaction with Mip6p.

Discussion

How cellular RNA is exported from the nucleus into the cytoplasm is still poorly understood. We report here the identification of a novel cellular factor for nuclear export of polyadenylated RNA. Mex67p was found genetically through a synthetic lethal screen using mutated *nup85*Δ. We showed recently that Nup85p, which is a member of the Nup84p complex, is not only involved in NPC biogenesis, but is also linked to the mRNA export machinery (Siniossoglou *et al.*, 1996). A conditional allele of *RAT9* which is allelic to *NUP85* also causes a strong and fast inhibition of mRNA export (Goldstein *et al.*, 1996). Therefore, the synergistic enhancement of defects in mRNA export, induced by mutations in both *mex67* and

nup85 could have caused synthetic lethality in the sl102 mutant. Conversely, Mex67p is not genetically interacting with Seh1p, another member of the Nup85p complex which does not participate in RNA transport (Siniossoglou *et al.*, 1996). Thus, Mex67p is genetically linked to the Nup85p complex as far as its mRNA export function is concerned. Accordingly, mex67 mutant cells do not reveal structurally distorted NPCs. The genes of two other synthetic lethal mutants derived from the screen with the *nup85*Δ allele have been recently cloned and shown to encode Nup188p and Nup170p (H.Tekotte and H.Santos-Rosa, unpublished data). Although both proteins were implicated to be involved in the organization of the structural core of the NPC (Aitchison *et al.*, 1995a; Nehrbass *et al.*, 1996; Zabel *et al.*, 1996), recent evidence suggested that Nup170p/Nle3p (Kenna *et al.*, 1996) and Nup188p (Anne de Bruyn Kops, personal communication) are also involved in mRNA export.

Evidence for a direct participation of Mex67p in nuclear mRNA export is: (i) the fast and efficient onset of an mRNA export defect in the ts mex67-5 mutant after shift to the restrictive temperature, with no apparent impairment in NLS-mediated nuclear protein import; and (ii) the physical interaction of Mex67p with the transport substrate which is polyadenylated RNA. The phenotype of nucleolar disintegration and partial inhibition of certain pre-rRNA processing steps in the mex67-5 mutant may be secondary, which could be due to a nucleolar depletion of newly synthesized ribosomal proteins or nucleolar components, as a cause of a general inhibition of mRNA export. It is known that a normal nucleolar structure requires ongoing ribosomal biogenesis (Oakes *et al.*, 1993) and nucleolar organization and rRNA processing are very sensitive to pleiotropic perturbations of diverse cellular functions. However, we cannot exclude that Mex67p is also involved in other export reactions including rRNA and snRNA transport.

In the electron microscope, several electron-dense aggregates scattered throughout the nucleoplasm can be seen in mex67-5 cells. Whether these are clustered RNP particles and correspond to the poly(A)$^+$ containing spots previously seen by *in situ* hybridization, is not clear. It will be interesting to determine whether in wild-type cells these foci represent the actual sites at which nuclear hnRNP export originates. The observation that, in ts mex67 cells, polyadenylated RNA does not accumulate at the NPCs, suggests that a transport step somewhere between the site of RNA transcription and the nuclear envelope is inhibited. Whether Mex67p is also required for intranuclear transport requires further clarification.

It is also not clear whether Mex67p shuttles between the nucleus and the cytoplasm, in order to fulfil its transport function, or if it performs its essential role exclusively at the nuclear pore complex. Wild-type Mex67p cannot be distinguished from a bona fide nucleoporin; however, mutant forms of Mex67p regain different subcellular locations and can be found both in the cytoplasm and nucleus; under these conditions of mislocalization, other tested nucleoporins such as Nsp1p and Nup85p remained bound to the NPCs. The association of Mex67p with the nuclear pores therefore could be transient and dynamic, and Mex67p may partition into the nucleus and cytoplasm. Similarly, Nup159p which is also involved in mRNA export in yeast has been reported to dissociate from NPCs when mutated (Gorsch *et al.*, 1995). We found a fraction of Mex67p physically bound to the purified Nup85p complex. However, this is only a minor pool, suggesting that this interaction could be transient. Finally, Mex67p–GFP still localizes to the NPCs in the nup85Δ mutant, showing that the N-domain of Nup85p is not involved in the targeting of Mex67p to the NPCs (A.Segref, unpublished results).

Recently, an RNA-export factor in yeast named Gle1p which contains a NES-like sequence active in heterologous systems has been identified and shown to interact with Rip1p and Nup100p (Murphy and Wente, 1996). Mex67p also contains a short peptide which not only resembles the NES of HIV Rev (Gerace, 1995; see also Figure 6A), but also acts as a NES in the *Xenopus* oocyte system. However, excess of Mex67p NES-like peptides microinjected into *Xenopus* oocyte nuclei did not inhibit the cellular mRNA export pathway, whereas U1ΔSm RNA export and the RRE-dependent RNA export was impaired. Therefore, the NES-resembling sequence in its native context within the folded Mex67p protein may perform another or an additional role in yeast. It should be mentioned in this context that proteins in *C.elegans* and human which are homologous to Mex67p have corresponding peptides which do not conform to the NES consensus (Figure 1B). Thus, the NES-resemblance and NES-function in the *Xenopus* system may be fortuitous in the case of the Mex67p sequence. Nevertheless, this short essential sequence plays a crucial role for Mex67p function since it is required for both mRNA export and association with nuclear pores.

Mex67p is not only a nuclear pore-associated protein, but has also physical contact to polyadenylated RNA in the living cell. One possibility is that Mex67p binds directly to RNA. However, Mex67p does not exhibit motifs indicative of an RNA-binding protein. It is also conceivable that Mex67p associates with RNA via (a) bona fide RNA-binding protein(s). HnRNP proteins, which shuttle between the nucleus and the cytoplasm, were implicated to be mediators of mRNA export (Piñol-Roma and Dreyfuss, 1992; Michael *et al.*, 1995; Lee *et al.*, 1996). Several hnRNP proteins were identified in yeast, including Nab1p/Npl3p/Nop3p, Nab2p and Nab3p (Wilson *et al.*, 1994; Russell and Tollervey, 1995; Lee *et al.*, 1996). When affinity-purified Mex67p–ProtA was analysed on Western blots, only trace amounts of Nab1p/Npl3 were present, and no Nab2p and Nab3p could be detected (data not shown). However, we can not exclude that Mex67p binds to these or other as yet unidentified hnRNP proteins, but this interaction is transient or not stable during biochemical purification. In an attempt to identify such proteins, a two-hybrid screen was performed. In this screen, Mip6p (Mex67-interacting protein) was found which is a putative RNA-binding protein with three RNP consensus motifs in its central part (see also Figure 9B). Mip6p is highly homologous to another yeast RNA-binding protein called Pes4p, which was found as a suppressor of DNA-polymerase ε subunit (accession No. P39684).

Although we cannot exclude a three-hybrid interaction between Mex67p and Mip6p involving a bridging RNA molecule, we find this less likely, because Mip6 lacking

Table I. Yeast strains

Strain	Genotype
RS453	Mat**a**/α,ade2/ade2,his3/his3,leu2/leu2,trp1/trp1,ura3/ura3
CH1462	Matα,ade2,ade3,his3,leu2,ura3 (Kranz and Holm, 1990)
nup85Δ	Mat**a**,ade2,his3,leu2,trp1,ura3,HIS3::nup85Δ(partial disruption/deletion)
RW nup85Δ	Matα,ade2,his3,leu2,ura3,HIS3::nup85Δ (pHT4467–URA3–ADE3–NUP85)
sl102	Matα,ade2,his3,leu2,trp1,ura3,HIS3::nup85Δ,mex67-102 (pHT4467–URA3–ADE3–NUP85)
MEX67 Disruption	Mat**a**/α,ade2/ade2,his3/his3,leu2/leu2,trp1/trp1,ura3/ura3,MEX67,mex67::HIS3
MEX67 shuffle	Mat**a** or α,ade2,his3,leu2,trp1,ura3,mex67:HIS3 (pRS316–URA3–MEX67)
MEX67–GFP	Mat**a**,ade2,his3,leu2,trp1,ura3,mex67:HIS3 (pUN100–LEU2–MEX67–GFP)
MEX67–ProtA	Mat**a**,ade2,his3,leu2,trp1,ura3,mex67:HIS3 (pUN100–LEU2–MEX67–ProtA)
mex67-5–GFP	Mat**a**,ade2,his3,leu2,trp1,ura3,mex67:HIS3 (pUN100–LEU2–mex67-5–GFP)
mex67-5–ProtA	Mat**a**,ade2,his3,leu2,trp1,ura3,mex67:HIS3 (pUN100–LEU2–mex67-5–ProtA)
mex67-5	Mat**a**,ade2,his3,leu2,trp1,ura3,mex67:HIS3 (pUN100–LEU2–mex67-5)
mex67–mut–nes1	Mat**a**,ade2,his3,leu2,trp1,ura3,mex67:HIS3 (pPR314–TRP1–mex67–mut–nes1)
mex67–mut–nes1–GFP	Mat**a**,ade2,his3,leu2,trp1,ura3,mex67:HIS3 (pRS314–TRP1–mex67–nes1–GFP)
mex67–mut–nes3–GFP	Mat**a**,ade2,his3,leu2,trp1,ura3,mex67:HIS3 (pRS314–TRP1–mex67–nes3–GFP)
nup84^{-}	Mat**a**,ade2,his3,leu2,trp1,ura3,nup84::HIS3
Y190	Mata,ade2,gal4,gal80,trp1,leu2,his3,ura3,LYS::GAL(UAS)–HIS3,URA3(UAS)–lacZ

the putative RNA binding domains (i.e. the carboxy-terminal part) still interacts with the Mex67p carboxy-terminal domain in the two-hybrid assay. We are currently investigating whether Mip6p represents a novel hnRNP or polyadenylate RNA binding protein in yeast which, together with Mex67p, is involved in nuclear mRNA export mechanisms.

The mex67-5 protein mislocalizes to the cytoplasm under restrictive growth conditions, suggesting that its association with nuclear pores is inhibited. Interestingly, we found the *CDC5* kinase gene as a high copy number suppressor of the mex67-5 mutation (A.Segref and E.C.Hurt, unpublished results). It is therefore possible that the function of Mex67p is regulated by phosphorylation. Cdc5p may not be the genuine kinase involved in the regulation of Mex67p, since Cdc5p is a mitotic kinase which acts at the G_2/M boundary and was frequently found in high-copy suppressor screens (Kitada *et al.*, 1993). However, it is possible that overproduced Cdc5p kinase can phosphorylate mutated mex67-5p, thereby curing the thermosensitive growth phenotype. It will be interesting to find out whether phosphorylation/dephosphorylation is a mechanism to control the Mex67p function and/or location.

In summary, we have identified Mex67p as a novel component of the RNA transport machinery in yeast. This export factor for polyadenylated RNA, which has related proteins with similar domain organization in human and *C.elegans*, is associated with the nuclear pores and interacts physically with polyadenylated RNA. However, the location of Mex67p at the NPCs may be dynamic. Accordingly, Mex67p is likely to directly participate in the export of mRNA from the nucleus to the cytoplasm.

Materials and methods

Yeast strains, DNA recombinant work and microbiological techniques

All strains used in this work are shown in Table I. Microbiological techniques, plasmid transformation, plasmid recovery, gene disruption, mating, sporulation of diploids and tetrad analysis were done essentially as described by Siniossoglou *et al.* (1996). Manipulation and analysis of DNA such as restriction analysis, end-filling, ligations, PCR amplifications and DNA sequencing were performed according to Maniatis *et al.* (1982). When constructs were generated by PCR, DNA which was derived from a PCR amplification was routinely sequenced.

Plasmids

The following plasmids were used in this study: pUN100: *ARS1/CEN4* plasmid with the *LEU2* marker (Elledge and Davis, 1988); pRS314 and pRS316: *ARS4/CEN6* plasmids with the *TRP1* and *URA3* marker, respectively (Sikorski and Hieter, 1989); YDp-H: pUC9-based plasmid with the *HIS3* marker (Berben *et al.*, 1991); pHT4467–URA3–ADE3: the *ADE3* gene derived from pCH1122 (Kranz and Holm, 1990) was inserted into the *Sma*I–*Spe*I site of plasmid pRS316; pHT4467–URA3–ADE3–NUP85: the *NUP85* gene was inserted as a *Xba*I–*Sac*I fragment into the *Xba*I–*Sac*I site of the polylinker of pHT4467.

Further plasmids, which are described in the text, were:

pUN100–LEU2–MEX67, pUN100–LEU2–mex67-5,
pUN100–LEU2–MEX67–ProtA, pUN100–LEU2–mex67-5–ProtA,
pUN100–LEU2–mex67-5–GFP, pUN100–LEU2–MEX67–GFP
pRS316–URA3–MEX67, pHT4467–URA3–mex67-5
pRS316–URA3–mex67Δnes, pRS314–TRP1–MEX67,
pRS314–TRP1–mex67Δnes, pRS314–TRP1–mex67-5,
pRS314–TRP1–mex67–nes1, pRS314–TRP1–mex67–nes2,
pRS314–TRP1–mex67–nes3, pRS314–TRP1–mex67–nes1–GFP,
pRS314–TRP1–mex67–nes3–GFP, pBluescript–HIS3::mex67,
pet8c–$(HIS)_6$–MEX67, pRS316–URA3–Matα2–lacZ.

Isolation of synthetic lethal mutants starting with the nup85Δ allele and cloning of MEX67

A screening strain was constructed for the red/white colony sectoring assay (Wimmer *et al.*, 1992) which contained the plasmid pHT4467–URA3–ADE3–NUP85 in a *HIS3::nup85Δ/ade2/ade3* genetic background. This screening strain RW nup85Δ was generated by mating strains nup85Δ with CH1462 (Kranz and Holm, 1990) followed by tetrad analysis (Table I). UV-mutagenesis was carried out as described earlier (Wimmer *et al.*, 1992; Grandi *et al.*, 1995). Approximately 15 000 surviving colonies were analysed for a red, non-sectoring phenotype at 30°C. 13 colonies finally fulfilled the requirement to be synthetically lethal with *nup85*Δ, but not with wild-type *NUP85*. Of the 13 sl mutants, sl102 (Table I) was transformed with a yeast genomic library inserted into pUN100–LEU2 as described earlier (Grandi *et al.*, 1995), and the complementing plasmid was recovered from transformants which regained both a red/white colony sectoring phenotype and growth on 5-FOA. The ORF of the *MEX67* gene was completely disrupted by inserting the *HIS3* gene (obtained as *Bam*HI fragment from plasmid YDp-H) between the ATG start codon and the stop codon. This insertion was possible, because *Bam*HI restriction sites were previously generated by PCR-mediated mutagenesis both at the start and stop codon. The linearized *mex67::HIS3* construct was used to transform the diploid yeast strain RS453. Heterozygous *mex67::HIS3* transformants with the integrated null allele were sporulated and tetrad analysis was done. No haploid progeny were growing which contained the *mex67::HIS3* null allele. The non-growing progeny normally germinated, but died in a 1–

2 cell stage. However, haploid *mex67::HIS3* cells formed colonies when they carried the *URA3*-containing plasmid with the *MEX67* gene. Finally, strain *mex67::HIS3* complemented by pURA3–MEX67 died on 5-FOA-containing plates, proving that *MEX67* is essential for vegetative growth.

Generation of thermosensitive mex67 mutants

Mutagenesis of double-stranded plasmid DNA containing the *MEX67* gene (pUN100–MEX67) was done with hydroxylamine essentially after Amberg *et al.* (1993). Mutagenized plasmid DNA was directly transformed into the MEX67 shuffle strain. A total of 3300 transformants were picked and plated at 23°C (permissive temperature) on 5-FOA-containing SDC plates. After 4 days, growing colonies (lacking pURA3–MEX67 and being complemented by a mutagenized pUN100–LEU2–mex67) were replica-plated on glucose-containing YPD plates both at 23°C and 37°C. From this screen, in total three ts mutants (ts mex67-1, mex67-4 and mex67-5) were obtained. Recovery of plasmid DNA from the cells was achieved by isolating total DNA and re-transformation of competent *Escherichia coli* MC1061 cells. The DNA corresponding to ts *mex67* allele was entirely sequenced. All three plasmids pUN100–mex67-1, pUN100–mex67-4 and pUN100–mex67-5 were retransformed in the MEX67 shuffle strain and after FOA-selection, the phenotype of recovered *mex67* ts alleles could be reproduced.

Construction of MEX67 fusion genes

The ProtA tag was derived from *Staphylococcus aureus* protein A and consisted of two IgG binding domains (Grandi *et al*., 1993, 1995). For the ProtA tagging of *MEX67*, a new *Bam*HI site was generated at the 3′ end of *MEX67* gene, six nucleotides before the stop codon. The DNA sequence around the stop codon is TTT GTG CAG TTC GGA TCC TAA TGA TAT TGT. A *Bam*HI fragment encoding the ProtA tag (Siniossoglou *et al.*, 1996) was inserted in frame and in the correct orientation at this newly generated *Bam*HI site of *MEX67*. The fusion gene *MEX67–ProtA* was inserted into the pUN100–LEU2 vector. To tag *MEX67* with the Green Fluorescent Protein (GFP), a *Bam*HI DNA fragment was amplified by PCR which encodes the *GFP* tag and inserted in frame into the *Bam*HI site previously generated at the stop codon of *MEX67* (see also above). In a similar way, also the ts *mex67-5* allele was tagged with the *GFP*. The GFP used is a S65T/V163A variant exhibiting enhanced fluorescence properties (Kahana and Silver, 1996; Shibasaki *et al.*, 1996).

Analysis of synthetic lethality between mex67 and other mutant alleles

To test for synthetic lethality with *nup85* mutant alleles, sl 102 was transformed with pRS314–TRP1–mex67-5 and transformants were streaked on 5-FOA plates. To test for synthetic lethality with *NUP84*, a strain carrying the *nup84::HIS3* null disruption was mated to MEX67 shuffle strain transformed with pRS314–TRP1–mex67-5. After sporulation and tetrad analysis, complete tetrads revealing a 2:2 HIS^+/his^- segregation and carrying both pRS316–URA3–MEX67 and pRS314–TRP1–mex67-5 were plated on 5-FOA-containing plates. In a similar way, matings and tetrad analysis between the MEX67 shuffle strain with strains seh1::HIS3 (Siniossoglou *et al.*, 1996) and $pom152^-$ (Wozniak *et al.*, 1994) were performed to determine possible synthetic lethal interactions (data not shown).

In vivo analysis of the location Mex67–GFP

The *in vivo* fluorescence analysis of cells expressing GFP-fusion proteins was done as recently described (Belgareh and Doye, 1997). Strains expressing GFP-fusion proteins were also transformed with an *ADE2*-containing pASZ11–ADE2 plasmid (obtained from B.Séraphin, EMBL, Heidelberg, Germany) to revert the red colour phenotype of ade2 strains which gives a strong vacuolar autofluorescence in the fluorescence microscope. Transformed cells growing in selective medium at the indicated temperatures were then examined for the GFP fluorescence signal in the fluorescein channel of a True Confocal Scanner LEICA TCS 4D confocal fluorescence microscope.

Mutational analysis of the NES-resembling motif within the Mex67p carboxy-terminal domain

The mutations within the sequence of Mex67p resembling the Rev NES were made by PCR-mediated site-specific mutagenesis. All PCR-derived DNA sequences were sequenced to confirm the generation of the desired mutation and to exclude additional PCR errors. To tag the mutated Mex67p forms with GFP, a *Bam*HI DNA fragment was amplified by PCR which encodes the *GFP* tag and inserted in frame into a *Bam*HI site previously generated at the stop codon of *MEX67* (see also above). The various fusion genes tagged with *GFP* were inserted into the pRS314–TRP1 vector and together with the pASZ11–ADE2 plasmid transformed into the MEX67 shuffle strain. Transformants were then selected on 5-FOA plates before the *in vivo* location of the GFP-fusion proteins was determined by fluorescence microscopy (see also above).

Generation of anti-Mex67p antibodies

The *MEX67* ORF was PCR-amplified using two primers that generated a *Sal*I site at the ATG start codon and a *Mlu*I site in the 3′-untranslated region of the gene. This ORF was then cloned into a pET–HIS6 vector as described earlier (Simos *et al.*, 1996). The recombinant Mex67p protein produced in *E.coli* was excised from SDS–polyacrylamide gels and injected into rabbits. From the immune serum, antibodies were affinity-purified on nitrocellulose strips containing the recombinant Mex67p antigen.

UV crosslinking of Mex67p to polyadenylated RNA

Isolation of UV-crosslinked polyadenylated RNA–RNP complexes from BJ926 yeast cells and analysis of crosslinked proteins including Mex67p, Nab1p/Npl3p, Nop1p, Nup85p and Nup57p by SDS–PAGE and Western blotting were done essentially as described (Anderson *et al.*, 1993; Russell and Tollervey, 1995). 500 ml of BJ926 cells grown to OD_{600} of 1.0 were harvested by centrifugation and treated further as described in Anderson *et al.* (1993). In a first step, the oligo(dT)-cellulose column which was loaded with either UV-crosslinked or non-crosslinked yeast cell lysate, was repeatedly washed with binding buffer before elution with 0.05% SDS-buffer. This first eluate was heated up to 65°C for 10 min, before it was diluted to 40 ml with binding buffer. The eluted $poly(A)^+$ RNA was reloaded on a second oligo(dT)-cellulose column and a second flow-through was collected. It was finally eluted with elution buffer and the RNA in the eluate was concentrated by butanol precipitation. After RNase T_1/T_2 treatment, aliquots of the first and second flow-through and the final eluate were analysed by SDS–polyacrylamide gel electrophoresis and Western blotting.

Two-hybrid screen

A DNA fragment encoding part of the P/Q/G-domain (starting at an internal *Nco*I site) plus the entire carboxy-terminal domain of Mex67p [residues 528–599; called pAS2-MEX67 (II)] was fused in frame to the *GAL4*-DNA binding domain present in the pAS2–TRP1 bait vector (Durfee *et al.*, 1993). As prey, a yeast genomic library fused to the *GAL4* activating domain and inserted into pACTII–LEU2 (called FRYL library; Fromont-Racine *et al*., 1997) was used in the two-hybrid screen. It was screened in the yeast strain Y190 for colonies which can grow on SDC (–leu –trp –his) plates containing 15 mM 3-AT and exhibit a $LacZ^+$ phenotype (X-Gal assay) according to Durfee *et al.* (1993). Of the 1.5×10^6 transformants, two clones finally fulfilled the requirements to specifically interact with Mex67p in the two-hybrid screen. One of these two clones, called *MIP6*, was further analysed and shown to encode a putative RNA-binding protein (accession No. YHR015W, 659 amino acids). The re-isolated pACTII–MIP6 (273) plasmid (prey; derived from the two-hybrid screen) was co-transformed with pAS2–MEX67 (II) bait plasmid into strain Y190 (*gal4, gal80, trp1, leu2, his3, UAS_{GAL}–LacZ*). For control reasons, other bait/prey combinations were also tested, including pAS2–MEX67 (II)/pACTII–NUP2 and pAS2–LOS1/pACTII–MIP6 (273) (K.Hellmuth, unpublished data). In each case, four transformants growing on SDC (–leu –trp) were streaked on SDC (–leu –trp –his; + 15 mM 3-AT; + X-Gal) plates. For control, further MEX67 constructs in pAS2 were made: (I) amino acids 483–599; (III), amino acids 549–599. Finally, a shortened MIP6 construct ranging from residues 385–659 was inserted into pACTII [called pACTII-MIP6 (385)].

Miscellaneous

Analysis of $poly(A)^+$ RNA export by *in situ* hybridization using fluorescently labelled oligo (dT) probes (Fabre *et al.*, 1994) and of nuclear protein import using the Matα2–lacZ and GAL::L25 NLS–ProtA–DHFR nuclear reporter constructs was done as recently described (Nehrbass *et al.*, 1993). Another assay for nuclear protein import was performed with the ts mex67-5 mutant according to Shulga *et al.* (1996) which allows *in vivo* measurement of the rate of nuclear import of a GFP reporter fused to the SV40 NLS. Purification of Mex67–ProtA fusion proteins under non-denaturing conditions and SDS–PAGE and Western blot analysis were performed essentially after Siniossoglou *et al.* (1996). To detect hnRNP proteins in eluates of the purified Mex67p–ProtA fusion protein by Western blotting, anti-Nab1p/Npl3 antibodies (a rabbit polyclonal immune serum), monoclonal anti-Nab2p and anti-Nab3p antibodies were used in 1:1000, 1:400 and 1:400 dilutions,

respectively. To detect ProtA-fusion proteins and nucleoporins, goat anti-rabbit IgG and mAB414 were used as first antibody (Siniossoglou *et al.*, 1996). Electron microscopy of fixed and thin-sectioned yeast cells was achieved according to Doye *et al.* (1994). The examination of rRNA processing defects in ts mex67 cells was done by Northern analysis (Tollervey *et al.*, 1993). The *in vivo* assay for loss of suppressor tRNA activity and the analysis of tRNA splicing was identical to that described in Simos *et al.* (1996). NES-activity measurements in the *Xenopus* oocyte system were done as described earlier (Fischer *et al.*, 1995) and the peptides used to test for NES activity in *Xenopus* oocytes were synthesized and HPLC-purified (R.Frank, ZMBH, Heidelberg, Germany).

Acknowledgements

We thank Cherichen Tekotte (EMBL, Heidelberg) for excellent technical assistance in the initial phase of this project, Klaus Hellmuth for the Los1p and Nup2p bait and prey constructs, David Tollervey (EMBL, Heidelberg) for help and advice, David Goldfarb (Rochester, New York, USA) for providing the reagents of the NLS–GFP *in vivo* import assay, Rick Wozniak (University of Alberta, Edmonton, Canada) for the pom152::HIS3 strain, Maurice Swanson and Anette Obermann (University of Florida, Gainesville, USA) for monoclonal anti-Nab2p (3F2) and Nab3p (AFL2) antibodies, Christian Siebel and Chris Guthrie (UCSF, San Francisco, USA) for polyclonal anti-Nab1p/Npl3p antibodies, Dr Pierre Legrain (Pasteur Institute, Paris) for the FRYL yeast genomic library and Dr Brigitte Lavoie (University of Geneva, Switzerland) for critical reading of the manuscript. E.C.H. is the recipient of grants from the Deutsche Forschungsgemeinschaft (SFB352) and the Eurofan/TAPIR network. K.S. is supported by a predoctoral fellowship from Boehringer Ingelheim Foundation for biomedical research.

References

Aitchison,J.D., Rout,M.P., Marelli,M., Blobel,G. and Wozniak,R.W. (1995a) Two novel related yeast nucleoporins Nup170p and Nup157p: complementation with the vertebrate homologue Nup155p and functional interactions with the yeast nuclear pore-membrane protein Pom152p. *J. Cell Biol.*, **131**, 1133–1148.

Aitchison,J.D., Blobel,G. and Rout,M.P. (1995b) Nup120p: a yeast nucleoporin required for NPC distribution and mRNA transport. *J. Cell Biol.*, **131**, 1659–1675.

Amberg,D.C., Goldstein,A.L. and Cole,C.N. (1992) Isolation and characterization of *RAT1*: an essential gene of *Saccharomyces cerevisiae* required for the efficient nucleocytoplasmic trafficking of mRNA. *Genes Dev.*, **6**, 1173–1189.

Amberg,D.C., Fleischmann,M., Stagljar,I., Cole,C.N. and Aebi,M. (1993) Nuclear PRP20 protein is required for mRNA export. *EMBO J.*, **12**, 233–241.

Anderson,J.T., Wilson,S.M., Datar,K.V. and Swanson,M.S. (1993) NAB2: a yeast nuclear polyadenylated RNA-binding protein essential for cell viability. *Mol. Cell. Biol.*, **13**, 2730–2741.

Belgareh,N. and Doye,V. (1997) Dynamics of nuclear pore distribution as revealed by GFP-nucleoporin localization in living yeast cells. *J. Cell Biol.*, **136**, 747–759.

Berben,G., Dumont,J., Gilliquet,V., Bolle,P.-A. and Hilger,F. (1991) The YDp plasmids: a uniform set of vectors bearing versatile gene disruption cassettes for *Saccharomyces cerevisiae*. *Yeast*, **7**, 475–477.

Bogerd,H.P., Fridell,R.A., Madore,S. and Cullen,B.R. (1995) Identification of a novel cellular cofactor for the Rev/Rex class of retroviral regulatory proteins. *Cell*, **82**, 485–494.

Cheng,Y., Dahlberg,J.E. and Lund,E. (1995) Diverse effects of the guanine nucleotide exchange factor RCC1 on RNA transport. *Science*, **267**, 1807–1810.

Del Priore,S., Snay,C.A. and Cole,C.N. (1996) The product of the *Saccharomyces cerevisiae RSS1* gene, identified as a high-copy suppressor of the rat7-1 temperature-sensitive allele of the *RAT7/NUP159* nucleoporin, is required for efficient mRNA export. *Mol. Cell. Biol.*, **7**, 1601–1611.

Doye,V. and Hurt,E.C. (1995) Genetic approaches to nuclear pore structure and function. *Trends Genet.*, **11**, 193–199.

Doye,V., Wepf,R. and Hurt,E.C. (1994) A novel nuclear pore protein Nup133p with distinct roles in poly $(A)^+$ RNA transport and nuclear pore distribution. *EMBO J.*, **13**, 6062–6075.

Durfee,T., Becherer,K., Chen,P.-L., Yeh,S.-H., Yang,Y., Kilburn,A.E., Lee,W.-H. and Elledge,S.J. (1993) The retinoblastoma protein associates with the protein phosphatase type 1 catalytic subunit. *Genes Dev.*, **7**, 555–569.

Elledge,S.J. and Davis,R.W. (1988) A family of versatile centromeric vectors designed for use in the sectoring-shuffle mutagenesis assay in *Saccharomyces cerevisiae*. *Gene*, **70**, 303–312.

Fabre,E. and Hurt,E.C. (1994) Nuclear transport. *Curr. Opin. Cell Biol.*, **6**, 335–342.

Fabre,E., Boelens,W.C, Wimmer,C., Mattaj,I.W. and Hurt,E.C (1994) Nup145p is required for nuclear export of mRNA and binds homopolymeric RNA *in vitro* via a novel conserved motif. *Cell*, **78**, 275–289.

Fischer,U., Meyer,S., Teufel,M., Heckel,C., Lührmann,R. and Rautmann,G. (1994) Evidence that HIV-1 Rev directly promotes the nuclear export of unspliced RNA. *EMBO J.*, **13**, 4105–4112.

Fischer,U., Huber,J., Boelens,W.C., Mattaj,I.W. and Lührmann,R. (1995) The HIV-1 Rev activation domain is a nuclear export signal that accesses an export pathway used by specific cellular RNAs. *Cell*, **82**, 475–483.

Fritz,C.C., Zapp,M.L. and Green,M.R. (1995) A human nucleoporin-like protein that specifically interacts with HIV rev. *Nature*, **376**, 530–533.

Fromont-Racine,M., Rain,J.-C. and Legrain,P. (1997) Functional analysis of the yeast genome through exhaustive two-hybrid screens. *Nature Genetics*, in press.

Gerace,L. (1995) Nuclear export signals and the fast track to the cytoplasm. *Cell*, **82**, 341–344.

Goldstein,A.L., Snay,C.A., Heath,C.V. and Cole,C.N. (1996) Pleiotropic nuclear defects associated with a conditional allele of the novel nucleoporin Rat9p/Nup85p. *Mol. Biol. Cell*, **7**, 917–934.

Gorsch,L.C., Dockendorff,T.C. and Cole,C.N. (1995) A conditional allele of the novel repeat-containing yeast nucleoporin *RAT7/NUP159* causes both rapid cessation of mRNA export and reversible clustering of nuclear pore complexes. *J. Cell Biol.*, **129**, 939–955.

Grandi,P., Doye,V. and Hurt,E.C. (1993) Purification of NSP1 reveals complex formation with 'GLFG' nucleoporins and a novel nuclear pore protein NIC96. *EMBO J.*, **12**, 3061–3071.

Grandi,P., Schlaich,N., Tekotte,H. and Hurt,E.C. (1995) Functional interaction of Nic96p with a core nucleoporin complex consisting of Nsp1p, Nup49p and a novel protein Nup57p. *EMBO J.*, **14**, 76–87.

Görlich,D. and Mattaj,I.W. (1996) Protein kinesis – Nucleocytoplasmic transport. *Science*, **271**, 1513–1518.

Heath,C.V., Copeland,C.S., Amberg,D.C., Del Priore,V., Snyder,M. and Cole,C.N. (1995) Nuclear pore complex clustering and nuclear accumulation of poly$(A)^+$ RNA associated with mutation of the *Saccharomyces cerevisiae RAT2/NUP120* gene. *J. Cell Biol.*, **131**, 1677–1697.

Izaurralde,E., Lewis,J., Gamberi,C., Jarmolowski,A., McGuigan,C. and Mattaj,I.W. (1995) A cap-binding protein complex mediating U snRNA export. *Nature*, **376**, 709–712.

Kadowaki,T., Zhao,Y. and Tartakoff,A.M. (1992) A conditional yeast mutant deficient in mRNA transport from nucleus to cytoplasm. *Proc. Natl Acad. Sci. USA*, **89**, 2312–2316.

Kadowaki,T., Goldfarb,D., Spitz,L.M., Tartakoff,A.M. and Ohno,M. (1993) Regulation of RNA processing and transport by a nuclear guanine nucleotide release protein and members of the Ras superfamily. *EMBO J.*, **12**, 2929–2937.

Kadowaki,T., Hitomi,M., Chen,S. and Tartakoff,A.M. (1994) Nuclear mRNA accumulation causes nucleolar fragmentation in yeast *mtr2* mutant. *Mol. Biol. Cell*, **5**, 1253–1263.

Kahana,J. and Silver,P. (1996) Use of the *A. victoria* green fluorescent protein to study protein dynamics *in vivo*. *Curr. Prot. Mol. Biol.*, **9**, 722–728.

Kenna,M.A., Petranka,J.G., Reilly,J.L. and Davis,L.I. (1996) Yeast Nle3p/Nup170p is required for normal stoichiometry of FG nucleoporins within the nuclear pore complex. *Mol. Cell. Biol.*, **16**, 2025–2036.

Kitada,K., Johnson,A.L., Johnston,L.H. and Sugino,A. (1993) A multicopy suppressor gene of the *Saccharomyces cerevisiae* G1 cell cycle mutant gene dbf4 encodes a protein kinase and is identified as CDC5. *Mol. Cell. Biol.*, **13**, 4445–4457.

Kobe,B. and Deisenhofer,J. (1994) The leucine-rich repeat: a versatile binding motif. *Trends Biochem. Sci.*, **19**, 415–421.

Kranz,J.E. and Holm,C. (1990) Cloning by function: an alternative approach for identifying yeast homologs of genes from other organisms. *Proc. Natl Acad. Sci. USA*, **87**, 6629–6633.

Lee,M.S., Henry,M. and Silver,P.A. (1996) A protein that shuttles between the nucleus and the cytoplasm is an important mediator of RNA export. *Genes Dev.*, **10**, 1233–1246.

Li,O., Heath,C.V., Amberg,D.C., Dockendorff,T.C., Copeland,C.S., Snyder,M. and Cole,C.N. (1995) Mutation or deletion of the *Saccharomyces cerevisiae* RAT3/NUP133 gene causes temperature-dependent nuclear accumulation of Poly(A)$^+$ RNA and constitutive clustering of nuclear pore complexes. *Mol. Biol. Cell*, **6**, 401–417.

Maniatis,T., Fritsch,E.T. and Sambrook, J. (1982) *Molecular Cloning: A Laboratory Manual*. Cold Spring Harbor Laboratory Press, Cold Spring Harbor, New York.

Michael,W.M., Choi,M.Y. and Dreyfuss,G. (1995) A nuclear export signal in hnRNP A1: a signal-mediated, temperature-dependent nuclear protein export pathway. *Cell*, **83**, 415–422.

Moore,M.S. and Blobel,G. (1993) The GTP-binding protein Ran/TC4 is required for protein import into the nucleus. *Nature*, **365**, 661–663.

Murphy,R. and Wente,S.R. (1996) An RNA-export mediator with an essential nuclear export signal. *Nature*, **383**, 357–360.

Nehrbass,U., Fabre,E., Dihlmann,S., Herth,W. and Hurt,E.C. (1993) Analysis of nucleo-cytoplasmic transport in a thermosensitive mutant of the nuclear pore protein NSP1. *Eur. J. Cell Biol.*, **62**, 1–12.

Nehrbass,U., Rout,M.P., Maguire,S., Blobel,G. and Wozniak,R.W. (1996) The yeast nucleoporin Nup188p interacts genetically and physically with the core structures of the nuclear pore complex. *J. Cell Biol.*, **133**, 1153–1162.

Noble,S.M. and Guthrie,C. (1996) Identification of novel genes required for yeast pre-mRNA splicing by means of cold-sensitive mutations. *Genetics*, **143**, 67–80.

Oakes,M., Nogi,Y., Clark,M.W. and Nomura,M. (1993) Structural alterations of the nucleolus in mutants of *Saccharomyces cerevisiae* defective in RNA polymerase I. *Mol. Cell. Biol.*, **13**, 2441–2455.

Piñol-Roma,S. and Dreyfuss,G. (1992) Shuttling of pre-mRNA binding proteins between nucleus and cytoplasm. *Nature*, **355**, 730–732.

Pollard,V.W., Michael,W.M., Nakielny,S., Siomi,M.C., Wang,F. and Dreyfuss,G. (1996) A novel receptor-mediated nuclear protein import pathway. *Cell*, **86**, 985–994.

Rexach,M. and Blobel,G. (1995) Protein import into nuclei: association and dissociation reactions involving transport substrate, transport factors, and nucleoporins. *Cell*, **83**, 683–692.

Russell,I. and Tollervey,D. (1995) Yeast Nop3p has structural and functional similarities to mammalian pre-mRNA binding proteins. *Eur. J. Cell Biol.*, **66**, 293–301.

Shibasaki,F., Price,E.R., Milan,D. and McKeon,F. (1996) Role of kinases and the phosphatase calcineurin in the nuclear shuttling of transcription factor NF-AT4. *Nature*, **382**, 370–373.

Shulga,N., Roberts,P., Gu,Z., Spitz,L., Tabb,M.M., Nomura,M. and Goldfarb,D.S. (1996) In vivo nuclear transport kinetics in *Saccharomyces cerevisiae*: a role for Hsp70 during targeting and translocation. *J. Cell Biol.*, **135**, 329–339.

Sikorski,R.S. and Hieter,R. (1989) A system of shuttle vectors and yeast host strains designed for efficient manipulation of DNA in *Saccharomyces cerevisiae*. *Genetics*, **122**, 19–27.

Simos,G., Tekotte,H., Grosjean,H., Segref,A., Sharma,K., Tollervey,D. and Hurt,E.C. (1996) Nuclear pore proteins are involved in the biogenesis of functional tRNA. *EMBO J.*, **15**, 2270–2284.

Siniossoglou,S., Wimmer,C., Rieger,M., Doye,V., Tekotte,H., Weise,C., Emig,S., Segref,A. and Hurt,E.C. (1996) A novel complex of nucleoporins, which includes Sec13p and a Sec13p homolog, is essential for normal nuclear pores. *Cell*, **84**, 265–275.

Stutz,F., Neville,M. and Rosbash,M. (1995) Identification of a novel nuclear pore-associated protein as a functional target of the HIV-1 Rev protein in yeast. *Cell*, **82**, 495–506.

Stutz,F., Izaurralde,E., Mattaj,I.W. and Rosbash,M. (1996) A role for nucleoporin FG repeat domains in export of human immunodeficiency virus type 1 Rev protein and RNA from the nucleus. *Mol. Cell. Biol.*, **16**, 7144–7150.

Tollervey,D., Lehtonen,H., Jansen,R.P., Kern,H. and Hurt,E.C. (1993) Temperature-sensitive mutations demonstrate roles for yeast fibrillarin in pre-rRNA processing, pre-rRNA methylation, and ribosome assembly. *Cell*, **72**, 443–457.

Wilson,S.M., Datar,K.V., Paddy,M.R., Swedlow,J.R. and Swanson,M.S. (1994) Characterization of nuclear polyadenylated RNA-binding proteins in *Saccharomyces cerevisiae*. *J. Cell Biol.*, **127**, 1173–1184.

Wimmer,C., Doye,V., Grandi,P., Nehrbass,U. and Hurt,E. (1992) A new subclass of nucleoporins that functionally interacts with nuclear pore protein NSP1. *EMBO J.*, **11**, 5051–5061.

Wozniak,R.W., Blobel,G. and Rout,M.P. (1994) POM152 is an integral protein of the pore membrane domain of the yeast nuclear envelope. *J. Cell Biol.*, **125**, 31–42.

Zabel,U., Doye,V., Tekotte,H., Wepf,R., Grandi,P. and Hurt,E.C. (1996) Nic96p is required for nuclear pore formation and functionally interacts with a novel nucleoporin, Nup188p. *J. Cell Biol.*, **133**, 1141–1152.

Received on January 2, 1997; revised on February 19, 1997